THE UNIVERSITY OF CHICAGO

A REGULATORY RNA BASED GENOME-WIDE INVESTIGATION OF BRAF INHIBITOR RESISTANCE IN MELANOMA

A DISSERTATION SUBMITTED TO

THE FACULTY OF THE DIVISION OF THE BIOLOGICAL SCIENCES

AND THE PRITZKER SCHOOL OF MEDICINE

IN CANDIDACY FOR THE DEGREE OF

DOCTOR OF PHILOSOPHY

INTERDISCIPLINARY SCIENTIST TRAINING PROGRAM:

CANCER BIOLOGY

BY

WILLIAM DION WAGSTAFF JR.

CHICAGO, ILLINOIS

DECEMBER 2022

Copyright © 2022 by William Dion Wagstaff Jr.

All rights reserved

To my mom and best friend.
Geneal Wagstaff 1959-2021

Table of Contents

List of Figures

List of Tables

Acknowledgments

I joined my first lab as a sophomore in high school through the Research Internships and Science Education Program at Emory University under the mentorship of Dr. Victor Corces. It was in that lab where I fell in love with the process of scientific discovery and decided that I'd like to pursue an MD/PhD. My journey isn't quite yet complete, but this dissertation represents a major milestone along the way. Making it to this point would be impossible where it not for support from my community.

TC is the best mentor I could have ever asked for. He struck an amazing balance of giving me the tools to become an independent thinker while also encouraging everyone in the lab to collaborate with one another. Unlike many other mentors, TC made lab culture a priority. Celebrating holidays and birthdays were just as important as lab meetings and journal clubs. I'm incredibly thankful for everyone in the University of Chicago Molecular Oncology Lab (also known as the MOlab) past and present for welcoming me into such an amazing family. I enjoyed learning so much about Chinese food and culture and I look forward to seeing what each of you accomplish. Because TC emphasized that family environment, I felt an incredible amount of support from him and other lab members when my mom became ill.

I'm so thankful for all of the insight my committee provided me with this project. I was lucky to have two UChicago MSTP Alumns on my committee in Dr. Diana Bolotin and Dr. David Raleigh and two expert RNA biologists in Dr. Chuan He and, my chair, Dr. Tao Pan. Obviously the science in this project was very important, but I relied on their perspective when it came to briefly stepping away from my project to be with my mother.

When I decided to embark on such a long academic journey, I asked my friends and family to come along on the ride. What a ride it's been so far! Most of my family members don't really understand what it means to pursue an MD or a PhD much less both degrees. Though that's presented me with some challenges, I've always had an abundance of love and support. I could list each and every person's name whose support was integral to me making it here. Instead I'd like to note that this dissertation—though a milestone—is just the beginning. My best work is still ahead of me. And I'll push myself to reach my potential as a way to honor the sacrifice, love, and support that was poured into me by my friends, family, and mentors. More than my own accomplishments, I look froward to the day I can give back and pour that same love and support back into younger generations of family and communities that mean so much to me.

Chapter 1

Introduction

Portions of this dissertation are reproduced or adapted from the following publication: Wagstaff, William, et al. "Melanoma: Molecular genetics, metastasis, targeted therapies, immunotherapies, and therapeutic resistance." Genes & Diseases (2022) 9, 1608-1623.

1.1 Background

1.1.1 Melanoma is a common cancer diagnosed in both men and women

Primarily located in the stratum basale, melanocytes are neural crest derived cells responsible for the production of two distinct pigments, eumelanin and pheomelanin, via melanogenesis (Figure 1.1)[1]. Basal layer melanogenesis is responsible for skin pigmentation[2]. Active melanogenesis is often stimulated by exposure to UV radiation—most commonly through intense sun exposure—for the purpose of protecting neighboring cells from excessive UV mediated DNA damage. Melanin absorbs the UV light thereby preventing it from causing DNA damage to cells in the hypodermis. Melanin is produced in the melanocyte, packaged in the melanosome, and transported to keratinocytes where the melanin is exocytosed into the cytoplasm. Each melanocyte has an estimated 30 to 40 dendrites that allow for the transfer of melanosomes to keratinocytes[3]. The phenotypic differences in skin pigmentation can be explained by the size and number of melanosomes, the amount and distribution of the types of melanin, and the distraction of keratinocytes.

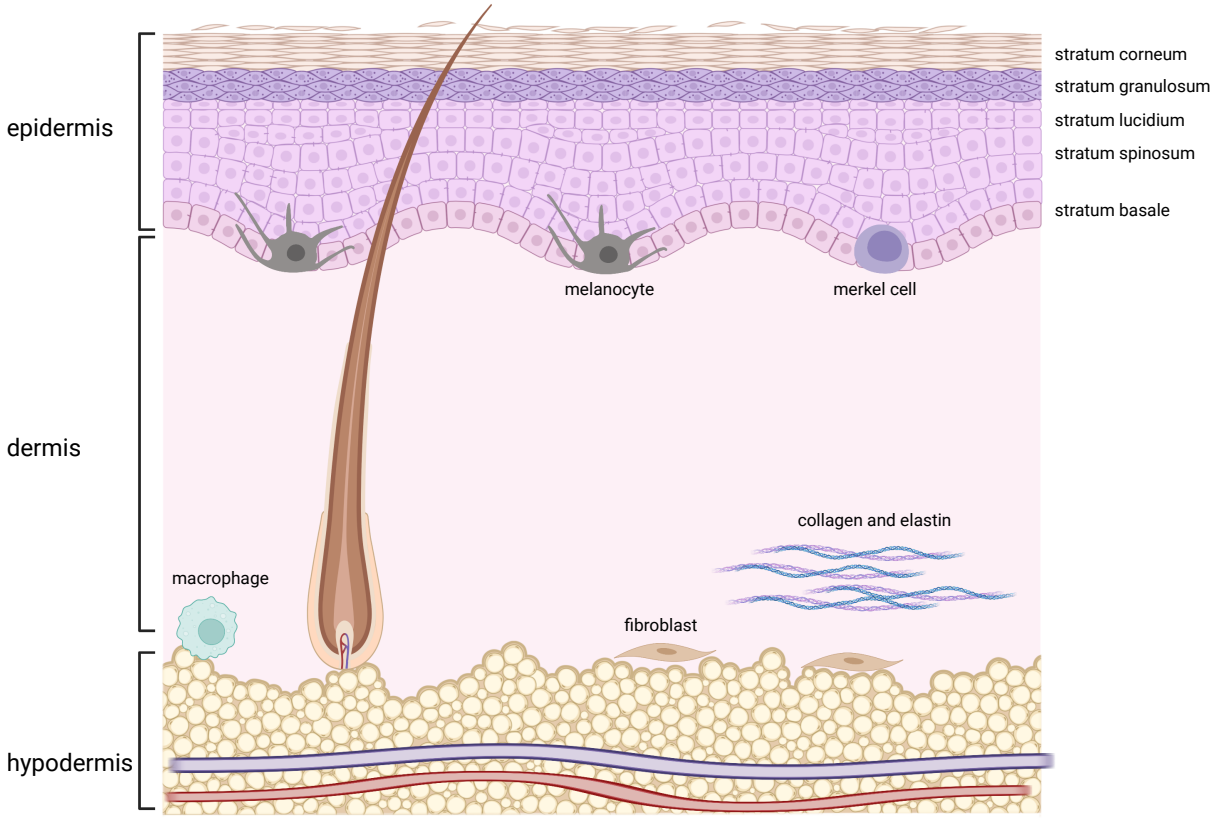

Figure 1.1. Diagram of the layers of the skin and their cellular and structural components

Changes to skin pigmentation that take place immediately following exposure to intense UV radiation are due to oxidation of previously existing melanin[4]. Whereas, longer term changes to skin pigmentation are due to increased eumelanin production. Though UV based DNA damage has the ability to induce malignant transformation of melanocytes, only a small percentage of melanomas are related to extrinsic UV radiation.

Cutaneous melanoma is a skin neoplasm resulting from the transformation and uncontrolled proliferation of melanocytes in the skin. Though rates are highest in the United States, Australia, and Europe, the global incidence of melanoma is high worldwide[5]. High incidence in those regions may be related to the fact that risk factors for melanoma include having fair features like blonde hair, lighter freckled skin, and blue or green eyes. The global incidence of melanoma is rising faster than any other solid tumor[6]. The rise in incidence is so drastic that melanoma is the 5th most common cancer worldwide in men and women[7]. Frequent exposure to UV light—both natural and synthetic—is also a risk factor. According to the American Cancer Society, invasive melanoma accounts for only 1% of all skin cancers but it's responsible for the vast majority of skin cancer related deaths[7]. The four major subtypes of melanoma are superficial spreading melanoma, lentigo maligna melanoma, acral lentiginous, and nodular melanoma (Figure 1.2). Superficial spreading melanoma accounts for about 70% of melanoma cases and is characterized by a slowly growing patch of dark skin[8]. This subtype usually occurs in lighter skinned patients and is typically found on the torso in men and the legs in women which is related to excessive UV exposure be it from the sun or tanning beds[8]. Lentigo maligna melanoma typically develops in older patients (>55 years) with sun damaged skin on the

face, ears, or neck[8]. Acral lentiginous melanoma is typically found in patients of color and presents as a dark spot on the sole of the foot or palms[9]. Acral lentiginous melanoma has its own subcategory called subungual melanoma that presents as dark vertical streaks under the nail beds of fingers and toes. It is the rarest form of melanoma and the only melanoma not associated at all with sun exposure. Nodular melanoma is the second most common form of melanoma making up about 15% of all cases[10]. It is considered the most aggressive of all the subtypes because it grows the fastest. What makes cutaneous melanoma more dangerous than other skin cancers—such as squamous cell carcinoma and basal cell carcinoma—is its ability to metastasize; especially after being diagnosed in late stage. Recently, the American Joint Committee on Cancer released updated staging parameters for melanoma[11]. A condensed version of these parameters are outlined in Table 1.1.

T Designation	Primary Tumor Thickness (mm)	N Designation	Regional Lymph Node	M Designation	Distant Metastasis
Tis	N/A	**Nx**	Lymph node cannot be assessed	**M0**	No metastasis
T1	≤1.0	**N1**	1 lymph node	**M1a**	Skin, cutaneous, distant lymph node
T2	1.0 - 2.0	**N2**	2 - 3 lymph nodes	**M1b**	lung
T3	2.0 - 4.0	**N3**	4+ lymph nodes	**M1c**	Other visceral sites
T4	≥4.0			**M1d**	Central nervous system

Stage	Primary Tumor (T)	Regional Lymph Node (N)	Distant Metastasis (M)
0	Tis	N0	M0
I	T1a - T2a	N0	M0
II	T2b - T4b	N0	M0
III	T0 - T4b	N1a - N3c	M0
IV	any T	any N	M1

Table 1.1. (A) TNM Staging (B) Pathological Staging[11]

Tis: the melanoma cells are only in the very top layer of the skin surface. It is called melanoma in situ.
T0: no melanoma cells can be seen where the melanoma star- ted (primary site).
T1: the melanoma is 1 mm thick or less. It is split into T1a and T1b.
T1a: the melanoma is less than 0.8 mm thick and the skin over the tumor does not look broken under the microscope (not ulcerated).
T1b: either: the melanoma is less than 0.8 mm thick but is ulcerated, or the melanoma is between 0.8 mm and 1.0 mm and may or may not be ulcerated.
T2: the melanoma is between 1 mm and 2 mm thick.
T3: the melanoma is between 2 mm and 4 mm thick.
T4: the melanoma is more than 4 mm thick.
T2 and T4 melanoma is further divided into a and b depending on whether it is ulcerated or not. A means without ulceration, b means with ulceration.
N0: there are no melanoma cells in the nearby lymph nodes. N1: there are melanoma cells in one lymph node or there are in- transit, satellite or microsatellite metastases.
N2: there are melanoma cells in 2 or 3 lymph nodes or there are melanoma cells in one lymph node and there are also in-transit, satellite or microsatellite metastases.
N3: there are melanoma cells in 4 or more lymph nodes or there are melanoma cells in 2 or 3 lymph nodes and there are in- transit, satellite or microsatellite metastases or there are

Table 1.1. Continued

melanoma cells in any number of lymph nodes and they have stuck to each other (matted lymph nodes).

M0: the cancer hasn't spread to another part of the body.

M1: the cancer has spread to another part of the body. M1 can be further divided depending on which parts of the body the cancer has spread to and whether there are raised levels of a chemical in the blood called lactate dehydrogenase (LDH).

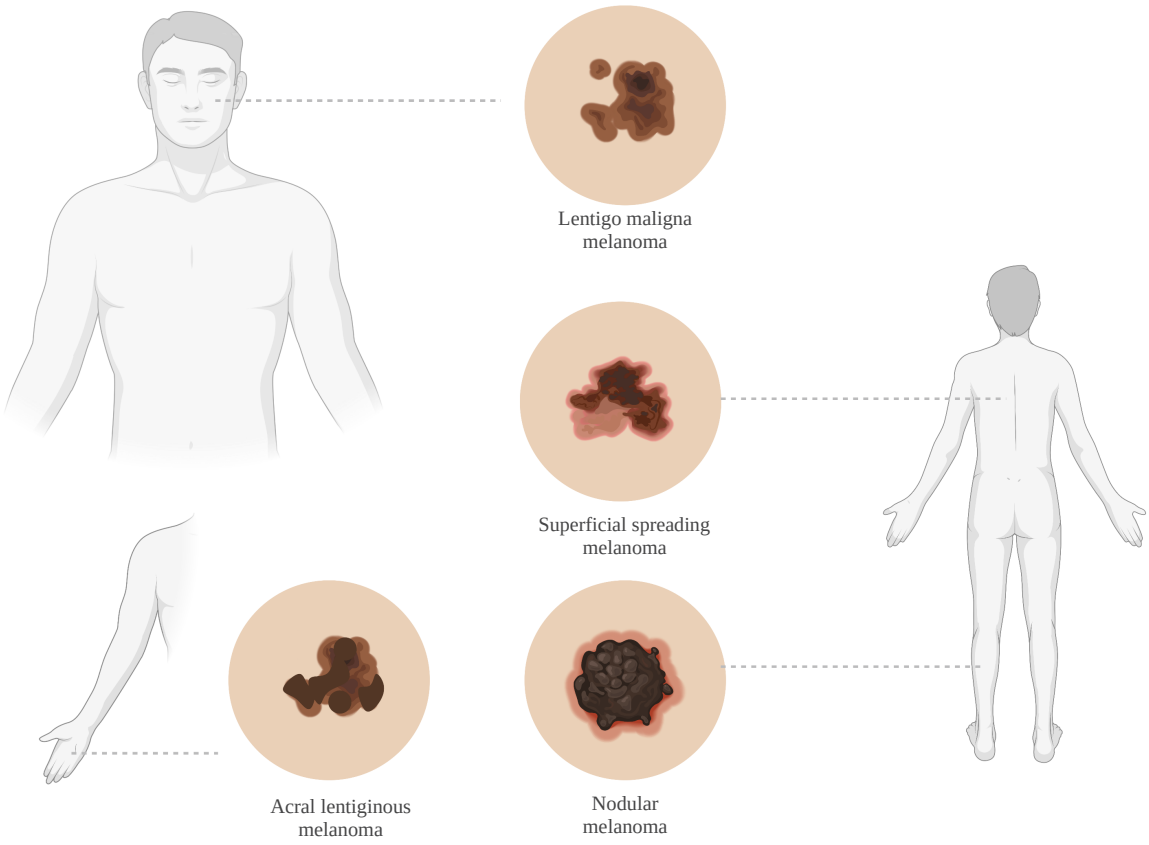

Figure 1.2. Diagram of the subtypes of cutaneous melanoma and their locations

1.1.2 The most common driver mutations of melanoma are well characterized

At physiologic levels, melanocytes undergo cell division two times per year on average. In order for a neoplasm to develop, mutations in cell division genes are necessary. So many genes are involved in cell division, but the ones that are associated with melanoma are well characterized.

As far as solid tumors are concerned, melanomas have high mutational burdens. Inherited melanoma is relatively rare with mutations in two genes being responsible for the 5 to 10% of cases[12]. Most of those cases are caused by mutations in the CDKN2A gene on chromosome 9; while only a handful of families have been identified as people who carry the CDK4 mutation on chromosome 12[12].

Since inherited melanoma is relatively rare, the mutational burden tends to be in somatic genes that regulate cell proliferation. Aberrant activation of the BRAF kinase occurs in ~50% of melanomas[12]. Over 90% of those mutations are due to point mutations at codon 600 that result in the substitution of glutamic acid for valine[13].

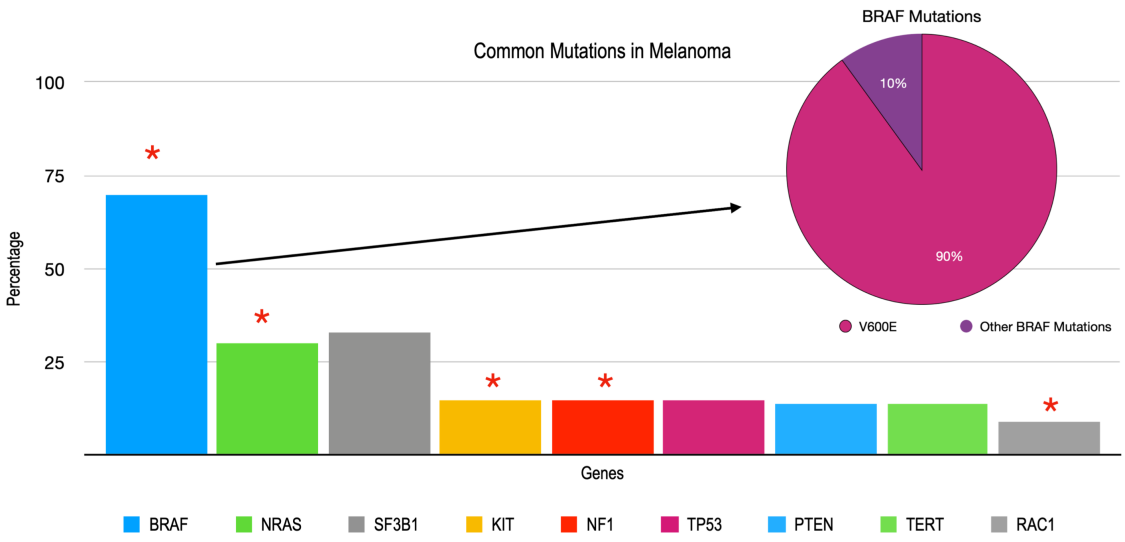

Figure 1.3. Common driver mutations in melanoma[15]
Red star indicates driver mutations associated with the MAPK signaling pathway

This constitutively active BRAF is not only implicated in tumor cell proliferation and survival, but it is also associated with increased tissue invasion, cell migration, metastasis, and evasion of the immune response. Furthermore, these mutations tend to be found in tumors that arise on skin without chronic sun induced damage.

Mutations in NRAS—a small GTPase—are found in around 20% of all melanomas with wild type BRAF[14]. 80% of those mutations are point mutations at position 61 that result in a glutamine-leucine substitution. This leads to defective GTPase activity, accumulation of RAS-GTP, and insensitivity to physiological regulation by guanine nucleotide exchange factors (GEFs) and GTPase activating proteins (GAPs). Melanomas that harbor NRAS mutations tend to be associated with more aggressive tumors and poor health outcomes[13]. This might be related to the fact that melanomas with NRAS mutations are more likely to have early initiation of the vertical growth phase[13]. Histologically, the lesions tend to be thicker and have higher mitotic activity with much lower rates of ulceration. However, there are higher rates of lymph node metastasis which may be related to increased cell motility and higher rates of epithelial mesenchymal transition (EMT) in NRAS mutated tumor cells[13].

Mutations in KIT1—a tyrosine kinase on the surface of the melanocyte—are found in about 3% of all melanomas[15]. Interestingly, KIT1 mutations tend to be mutually exclusive of mutations in either BRAF or NRAS. These independent activating mutations are spread across exons 9, 11, 13, and 17 and tend to be found in older patients with acral lentiginous subtypes as well as melanomas that are found in chronically sun damaged skin[16]. Mutant KIT is associated with several signaling pathways related to cell proliferation and metastasis[17].

Unlike KIT1, mutations in NF1 tend not to be mutually exclusive with BRAF or NRAS mutations[18]. This tumor suppressor gene—mutated in about 10 to 15% of melanomas—is responsible for producing a GAP that is known to regulate RAS by converting the active RAS-GTP to RAS-GDP[17]. These loss of function mutations are common in older (>55 years) patients with chronically sun damaged skin and tend to be found in the head and neck region[17]. Most typically, NF1 mutations are found in a rare histologic subtype of melanoma called desmoplastic melanoma that is characterized by fibroblast-like spindled melanocytes surrounded by an abundance of collagen fibers[19]. These melanomas tend to have higher relative mutational burden and mutations specially associated with UV exposure[18]. In spite of their high mutational burden, these melanomas tend to have thicker tumors that are associated with high rates of local recurrence but low rates of metastasis to regional lymph nodes. One study showed high rates of mutations in three other tumor suppressor genes: p53, PTPRT, and PTPRD[18]. However, NF1 mutant melanomas are associated with a better relative prognosis.

Activating mutations in RAC1 are found in about 9.2% of sun exposed melanomas[20]. These mutations carry a signature for UVB damage and are associated with wild type BRAF and NRAS and occur early in tumorigenesis. Unlike BRAF and NRAS mutations, these mutations are not found in benign nevi[19]. One group showed that functional studies of mutant RAC1 demonstrate a physiological GTPase activity with an increased inherent exchange of GTP for GDP[19]. This increase in exchange rate essentially categorizes this mutation as an oncogene.

Mutations in TERT are unique because the mutations are found in a promoter gene. In fact, TERT mutations are found in around 70% of melanomas[21]. The mutations—likely directly induced by UV damage—generate binding motifs for the ETS transcription factors that increase

TERT transcriptional activity anywhere from two to fourfold. The increase in transcriptional activity essentially results in an increase in telomerase production. Though insufficient in bypassing oncogene-induced senescence, aberrant TERT activation may contribute to immortality in transformed melanocytes[20]. Histologically, melanomas with TERT mutations tend to present as thicker lesions with high mitotic activity and all of these characteristics were found in tumors of older patients. Interestingly enough, TERT mutations alone were not associated with tissue invasion rates, tumor ulceration, tumor necrosis, primary tumor location, or reduced survival[22]. In one study, TERT mutations were associated with wild type BRAF, but the association was not statistically significant[21]. One hypothesis is that TERT mutations allow neoplastic cells to survive long enough to develop other more important driver mutations as the disease progresses.

All of the aforementioned mutations—with the exception of the TERT mutations—have the MAPK signaling pathway in common. This pathway is known driver of cell proliferation and the signaling cascade begins when a mitogen—like extracellular growth factor (EGF)—binds an extracellular receptor—like extracellular growth factor receptor (EGFR). That binding activates the tyrosine kinase domain of the intercellular portion of EGFR. Once phosphorylated, the cytoplasmic domain of EGFR binds docking proteins—like GRB2—that form complexes with GEFs—like SOS. Activated SOS removes GDPs from Ras allowing it to become activated by binding GTPs. GTP bound RAS acts as a protein kinase on BRAF. Phosphorylated BRAF acts as a protein kinase on MEK. Phosphorylated MEK acts as a protein kinase on ERK. Once ERK is phosphorylated, it translocates into the nucleus to act as a transcription factor for cell proliferation genes.

As far as treatment is concerned, this is a positive start given the MAPK signaling pathway is well described and several of its components could serve as possible therapeutic targets. Mutations in BRAF are both the most common overall mutations and the most homogenous.

1.1.3 Mutations that are associated with metastasis and advanced disease

The metastatic progression of melanoma can be guided by phenotypic drivers. A phenotypic driver of metastasis includes the stage-dependent regulation of anti-apoptotic proteins, such as the expression of BCL-2, which progressively decreases from the radial tumor growth phase to the vertical tumor growth phase while the expression levels of MCL1, BCL-XL, survivin (also known as BIRC5) and XIAP increase[23]. The role of differentiation factors in metastasis is largely controlled by microphthalmia-associated transcription factor (MITF) and canonical WNT signaling. MITF is a transcription factor central to melanocyte survival, proliferation, and melanin-pigment production[24]. MIFT amplification has been found in 21% of metastases compared to 10% of primary melanomas[25]. The WNT signaling through β-catenin promotes melanocytic differentiation through direct transcriptional upregulation of MIFT[26]. Oncogenic β-catenin mutations are thought to lead to constitutive activation of the canonical WNT pathway[27].

As previously mentioned, the mitogen-activated protein kinase (MAPK)/extracellular-signal-regulated kinase (ERK) pathway is the most mutated pathway in melanoma, with BRAF and NRAS being the most mutated components. Epidemiological observations from human melanomas suggest there is no difference in rates of metastasis between BRAF and NRAS

mutant melanomas, though both may exhibit higher rates of metastasis compared to RAS/RAF wild type melanomas[28,29,30]. The PI3K/AKT pathway is also frequently constitutively activated in melanoma through genetic or epigenetic inactivation of PTEN tumor suppressor and copy number gains or over-expression of AKT3[31,32,33]. The loss of PTEN and subsequent activation of PI3K/AKT pathway drives the metastasis of melanomas initiated by activating RAS and RAF mutations[34,35]. In these models, activation of PI3K/AKT is also critical in primary tumor formation, which makes it challenging to infer its specific role in metastasis. A recent study by Deng et al showed the expression of Wnt-inducible signaling protein 1 (WISP1), a downstream effector of the Wnt/β-catenin pathway, is increased in melanoma and associated with reduced overall survival in patients diagnosed with primary melanoma[36]. WISP1 is a soluble signal released by melanoma cells to reshape their microenvironment, enhanced tumor invasion, and metastasis by promoting an EMT-like process[35]. WISP1 specifically upregulates EMT transcription factors and mesenchymal markers and represses E-cadherin and MITF[35]. The role of WISP1 in melanoma has been previously studied in the context of fibroblasts and Notch signaling[37]. One hypothesis is that WISP1 is a downstream target of Notch signaling, an intercellular signaling cascade that is activated in human melanoma cells and is essential for their growth and metastasis.

1.1.4 Current standards of care for treating melanoma and their shortcomings

Although the surgical removal of tumors has proved to be effective in treating melanoma, the success of the surgery is highly dependent on the stage of the cancer. In the earlier stages of melanoma, prior to metastasis, the surgical resection of the tumor can be a successful treatment[38].

Once the cancer metastasizes, survival rates are significantly decreased when treated with surgical resection[37]. Prior to the use of immunotherapy, the five-year survival rate for metastatic melanoma treated with surgical resection was 15-20%[39]. Thus, the management of primary cutaneous melanomas can be handled by surgical resection whereas more advanced stages require additional therapeutic remedies[40]. Surgery is the optimal treatment for patients with melanoma tumors in stages I-IIIB, although procedures for the surgery will differ depending on the clinical features of the tumors[41].

The FDA approved dacarbazine, or dimethyltriazeno-imidazol carboxamide, in 1975 and it has served as both the first and only chemotherapeutic drug approved by the FDA for melanoma[39]. Dacarbazine works as an alkylating agent that generates methyl isothiocyanate (MITC) and exerts cytotoxic effects by preventing DNA replication[39]. Other single agent chemotherapies, including the microtubule inhibitor agent vindesine, have shown a response rate of under 20% when used alone[39]. The combination of dacarbazine and vindesine, however, have failed to show an increased response rate in metastatic melanoma patients[39]. More recently, dacarbazine no longer serves as the standard of care for metastatic melanoma due to its median survival from 5-11 months and 1-year survival rate of 27%[37]. To date, chemotherapy drugs have not been more effective in terms of survival rates, and none have been less toxic than dacarbazine[37]. Similarly, radiation therapy provides little clinical benefit as a treatment modality for melanoma due to the fact that melanoma is relatively radioresistant[42].

Inhibitors of BRAF (BRAFi) are the prototype targeted therapies that have met clinical successes, but also hampered by acquired resistance[43]. The BRAFV600E mutation is associated with sensitivity to a class of agents that block hyperactive BRAFV600E activity. The most

clinically effective BRAFi's are vemurafenib and dabrafenib. Although their significant clinical success is well documented, acquired resistance invariably occurs in most patients. Clinical data show acquired resistance develops as early as 2 months and as late as 18 months into treatment. It has been shown that resistance mechanism often involves reactivation of MAPK signaling. Though, BRAFV600E mutations account for more than 90% of BRAF mutations in melanoma, the drug that targets that mutant protein drives resistance by increasing activity of mutant BRAF monomers, increasing expression of PDGF receptors on the cell surface, increasing upstream NRAS mutations, and by increasing tumor cell sensitivity to HGF secreted by proximate stromal cells[44,45].

In spite of being the first oncogene identified in melanoma, treating melanomas with NRAS mutations has been extremely difficult. Farnesyl transferase inhibitors were designed to prevent post translational modification of RAS and its insertion into the plasma membrane thereby preventing RAS activation[46]. Non-specificity might have contributed to such a low impact on NRAS mutated tumors because so many membrane bound proteins are farnesylated. Salirasib is a small molecule that disrupts RAS localization at the plasma membrane resulting in death of RAS transformed cells[45]. This occurs via blocking RAS-GTP from binding galactin 1 on the plasma membrane. Salirasib has shown some promise at the preclinical level, though further investigation is required. Interfering RNAs are another tool used to target NRAS mutated melanomas. The approach has been validated in preclinical models, but delivery is a significant challenge due to the instability of nucleic acids in circulation.

Targeting downstream components of the MAPK signaling pathway with MEK inhibitors decreased resistance, but only in the short term. Although MEK acts downstream of RAF, there

is a relatively low incidence of MEK mutations in human cancers[47]. MEK inhibitors—like trametinib—that allosterically bind both MEK1 and MEK2 increased progression free survival in most patients[48]. However, acquired resistance to combination therapy eventually emerges. This suggests that tumor cells escape combination therapy downstream via ERK or upstream via the RAS-PI3K axis.

In the early 1900s Paul Ehrlich suggested that cancer rates would be higher were it not for the immune system[49,50]. More than a half century later, the immunosurveillance theory that suggested that the adaptive immune system is responsible for preventing cancer in immunocompetent hosts came to be. Since then, the hypotheses about how the role the immune system plays in cancer have become more developed and with that development came the advent of immunotherapy; the most effective of which are checkpoint inhibitors[40]. Generally speaking, checkpoint inhibitors are ligands that bind receptors that trigger signaling pathways that prevent or dampen an immune response to a pathogen.

First antibodies blocking CTLA-4 were developed to bias T cells toward activation. The next generation of checkpoint inhibitors were PD-1 and PD-L1 monoclonal antibodies that targeted the T cell and the tumor cell respectfully. Generally speaking, checkpoint inhibitors were extremely effective at unlocking the ability of effector T cells to reduce tumor burden. In early clinical trials, treatment with ipilimumab, the CTLA-4 blockade molecule, resulted in 1 and 2 year survival rates of 46% and 24% respectively. Treatment with PD-1 resulted in even better results. About 20% of melanoma patients treated with anti-PD-1 antibodies with and without the addition of anti-CTLA-4 antibodies experience complete remission. It is even understood that treatment can end after 6 months of therapy—thereby reducing side effects—because the chance

of relapse is estimated as less than 5% over 5 years in patients with a sustained response. However, one trial revealed that 82% of patients with stage IV melanoma had an incomplete response or their disease progressed following single agent or combination immunotherapy treatment[51].

Though checkpoint inhibitors have shown great clinical success, the extent of that success is truly found in a minority of patients. Many patients experience either primary resistance or acquired resistance to those therapies. Some of the difference in patient outcomes can be attributed to variance in the density of immune cells in the tumor tissue. Patients with hot tumors or tumors with high immune cell infiltrate tend to respond better to checkpoint blockade therapy than patients with cold tumors. Elevated serum LDH levels are associated with primary resistance as well. Increased LDH expression in the tumor microenvironment results in increased activation of immunosuppressive cell types like myeloid derived suppressor cells and tumor associated macrophages. Much less is understood about acquired resistance to checkpoint inhibitors.

In any case, treatment eventually results in a tumor cell population that is resistant to the drugs. One marker of that resistant population is low beta-2-microglobulin (B2M). B2M is required for functional MHC-1 expression and MHC-1 is required to present tumor antigen to cytotoxic T cells. Additionally, acquired resistance can develop as the result of additional immune checkpoint marker upregulation such as TIM-3, LAG-3, and HAVCR-2. This type of acquired resistance shows that blocking one pathway toward immunosuppression might result in activation of other immunosuppressive pathways.

1.1.5 Scope of Dissertation

BRAFi is the most effective treatment for advanced melanoma. The strong initial response to treatment that most tumors display is promising. The fact that drug resistance is almost inevitable provides the scientific community with an opportunity to understand the underlying mechanism behind resistance so that we may combat it. Clinical data demonstrate that targeting other components of the MAPK signaling pathway delays but does not prevent the resistant phenotype. This suggests that a more robust genetic approach may be more appropriate. The goal of this dissertation is to utilize a novel short artificial RNA (saRNA) library to identify a network of regulatory noncoding RNAs responsible for the development of BRAFi resistance in human melanoma.

In Chapter 2 we develop and characterize the retrovirus-based 19nt artificial RNA library that confers resistance to BRAFi. This chapter includes assessment of the biological relevance of our synthetic RNA library and contains the initial verification of the noncoding nature of the transcripts.

Chapter 3 highlights the broad transcriptomic differences between BRAFi resistant cell populations and parental cell populations. In this chapter, we identify specific transcripts that are enriched in resistant cell populations and confirm that individual transcripts confer resistance.

Chapter 4 examines how enrichment of BRAFi resistance-associated noncoding transcripts impacts exomic sequences of potential BRAFi resistance-associated genes. In this chapter we use whole exomic sequencing (WES) to analyze single nucleotide variant (SNV) changes across the genome in the resistant cell lines as compared to their parental cell lines. We also highlight similarities in changes in exomic sequences between different cell lines. Based on

our hypothesis, we also analyze the relationships between SNV changes and possible miRNA binding. At the conclusion of this chapter we integrate our analysis of Chapters 2 through 4 to create a possible mechanism of action that connects introduction of our short artificial RNA library as an innovative reverse genomic strategy to delineate the development of the BRAFi resistance phenotype in human melanomas.

Chapter 2

Establishing a biologically relevant short RNA library to probe acquired BRAFi resistance

2.1 Introduction

As previously mentioned in Chapter 1, molecular targeted therapies—specifically BRAFi's—are initially quite efficient when it comes to treating melanoma. However, resistance is a major and, often, inevitable obstacle. Targeted therapy resistance is a moving target that cannot be explained by mutations in one gene alone. Given that an estimated 2% of the genome is transcribed into mRNA, there is a high likelihood that noncoding RNA plays a crucial role in the epigenetic landscape of drug resistance. This is especially significant given that dysregulation of noncoding RNA is linked to all cancers and affects all major cancer hallmarks[52].

Noncoding RNAs can be generally separated into four large categories: ribosomal RNA, transfer RNA, short noncoding RNA, and long noncoding RNA[53]. Ribosomal RNAs are molecular building blocks that bind ribosomal proteins resulting in small and large ribosomal subunits. Transfer RNAs are responsible for shuttling amino acids to the ribosome in the protein polymerization process. Long noncoding RNA molecules are typically longer than 200 nucleotides and make up the largest class of noncoding RNAs. Long noncoding RNAs can be divided into the following: long intergenic ncRNAs, antisense RNAs, pseudogenes, and circular RNAs[54]. Short noncoding RNA are typically less than 200 nucleotides and can be divided into the following categories: microRNAs, siRNAs, snoRNAs, and piwi-interacting RNAs. Together, long and short noncoding RNAs interact with DNA, RNA, proteins, and micropeptides to induce epigenetic changes.

The role of noncoding RNA in melanoma tumorigenesis and metastasis has been probed. One group showed that the long noncoding RNA SPRY4-IT1 is differentially expressed in melanoma cells as compared to healthy melanocytes[55]. Knocking down that molecule with RNAi in vitro led to defects in cell growth, differentiation, and higher rates of apoptosis in melanoma cells[4]. Further more, higher transcription rates of SPRY4-IT1 in patient samples were found in the primary tumor as well as regional and distant metastatic sites[4]. Another group found that the long noncoding RNA molecule SLNCR1 was associated with an invasive phenotype in melanoma; allowing for an increased likelihood of metastasis[56]. When RNA sequencing was performed on short term culture of patient samples, increased expression of SLNCR1 correlated with reduced survival rates[5].

It is likely that short and long noncoding RNAs work in tandem to contribute to acquired targeted therapy resistance in melanoma. The miRNA, miR-211-5p, is the most differentially expressed miRNA between melanoma cell lines and normal melanocytes[57]. Transformed melanocytes down regulate miR-211-5p, which results in decreased MITF, a transcription factor responsible for transcription of enzymes specific to melanogenesis[6]. It has been demonstrated that melanocytes treated with vemurafenib express less pigmentation and that condition is reversed as the tumor cells develop resistance. Long noncoding RNAs such as BANCR further contribute to the development of melanoma by increasing cell proliferation via downstream ERK activation[58]. One group demonstrated that inhibition of SAMMSON in addition to treatment with dabrafenib resulted in tumor regression in patient derived melanoma xenograft models[59]. We even know that noncoding RNAs are directly involved in activating the MAPK signaling pathway in tumorigenesis. Over-expression of RP11-705C15.3—a regulator of miR-145-5p—

promoted melanoma cell proliferation, inhibited apoptosis, and promoted migration and invasion[60]. The interplay between short and long noncoding RNAs demonstrates that targeting both types of molecules will be necessary to combat acquired molecular targeted therapy resistance.

The mechanism of action of noncoding RNA in cancer drug resistance is unknown. However, the general mechanistic classifications of noncoding RNA can be separated into the following three categories: guide, dynamic scaffold, and decoy[61]. Noncoding RNAs have the ability to bind regulatory or enzymatically active proteins and direct them to precise loci in the genome[10]. They can also serve as a platform for the transient assembly of large protein complexes[10]. Lastly, noncoding RNAs can act as a sponge that binds regulatory factors; thus inhibiting them from acting on the genome. Additionally, noncoding RNAs have been shown to be secreted in exosomes by melanoma cells[62]. Those exosomes create a tumorigenic environment by modifying nearby stromal cells, increasing angiogenesis, creating a immunosuppressive tumor microenvironment, and by priming regional and distal lymph nodes for metastasis[11]. Together, these findings suggest that noncoding RNAs should be investigated for their role in targeted therapy resistance in melanoma.

2.2 Results

2.2.1 N19 Library design

In order to test our central hypothesis, we decided to generate a randomized 19mer short RNA library using the workflow shown in Figure 2.1.

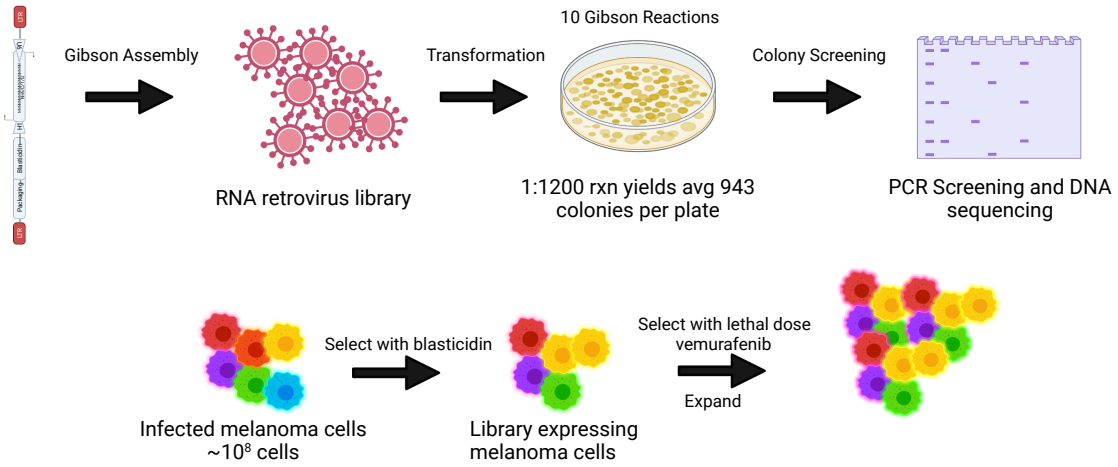

Figure 2.1. Workflow of the project

(A) The first stage of the project was to construct the randomized short N19 RNA library into a retroviral transfer vector through the Gibson Assembly method. The unique clones were grown up in bacterial cells and PCR confirmed the presence of the randomized N19 sequences. Then those inserts were validated by DNA sequencing. Next generation deep sequencing analysis revealed the library contains at least $3x10^7$ unique N19 sequences.

(B) The second stage of the project was to package the short RNA-expressing retrovirus library and infect melanoma cells, select for blasticidirn resistant cells, select for vemurafenib resistant cells, and expand those stably resistant cell populations.

In the genetically complex environment of targeted therapy resistance, we decided to design a library capable of delivering a massive number of noncoding RNA molecules (Figure 2.2).

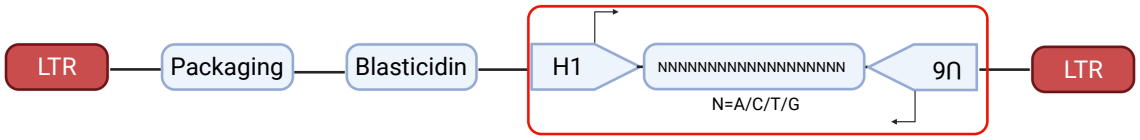

Figure 2.2. Plasmid map of the N19 RNA library
Highlighted in red is the randomized 19mer portion flanked on the left by the RNA Pol III promoters H1 (left) and U6 (right). These promoters were used to drive production of short 19nt noncoding RNA transcripts

Highlighted in red are the three crucial components of the plasmid. On the far left of the highlighted region is the H1 promoter. On the far right of the highlighted region is the U6 promoter. Both the H1 and U6 promoters are RNA polymerase III promoters used to bias transcription toward small noncoding RNAs. Including one in the sense direction and the other in the antisense direction allowed us to increase the number of single stranded RNA molecules that the plasmid produced. In between those two promoters is a randomized 19mer cassette. Deep sequencing confirmed that we were able to generate $3x10^7$ unique 19mer transcripts via Gibson assembly (Figure 2.3 A). We then took a random sampling of 30 colonies and used PCR to confirm retroviral delivery of the library (Figure 2.3 C). Those data revealed an estimated 90% plasmid delivery rate which is consistent with previous data generated by our lab. Sequencing 9 of those colonies showed that the 19mers were in fact random and unique (Figure 2.3 D). We then used the National Center for Biotechnology Information Basic Local Alignment Search Tool (NCBI BLAST) to determine if there were any complete matches to protein coding genes for each of the clones. Figure 2.3 E shows a representative search results from clone #1.

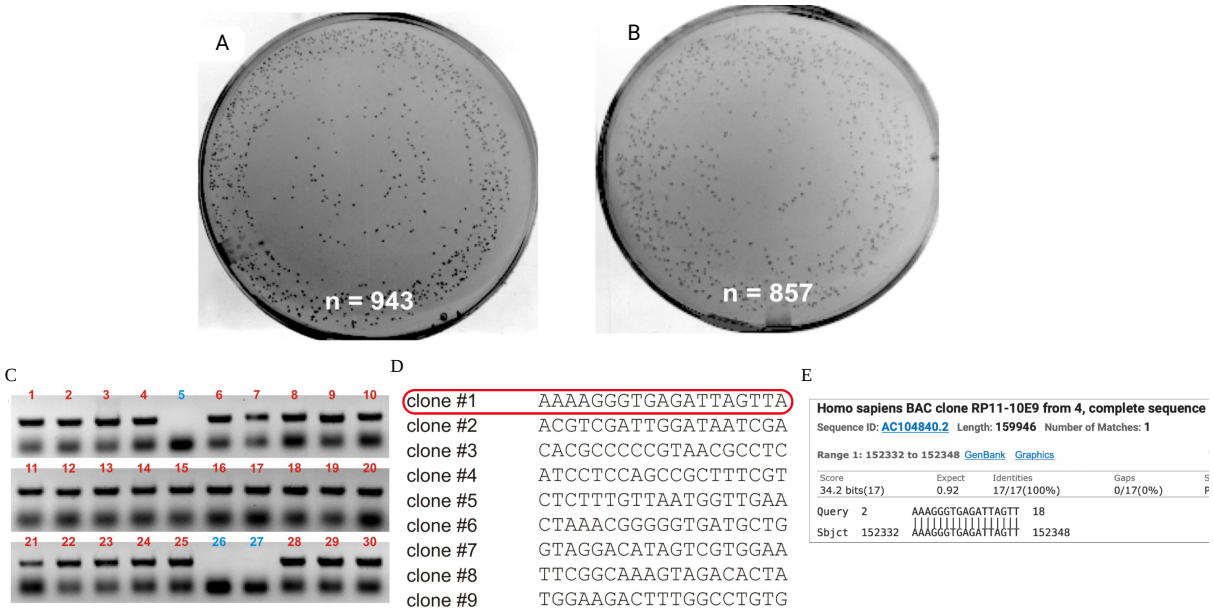

Figure 2.3. Confirmation of the positivity and uniqueness of the bacterial clones harboring the N19 library

(A) Bacterial plate with 100 µL of 1:1200 reaction with n = 943 colonies. (B) Bacterial plate with 100 uL of 1:1200 reaction with n = 857 colonies. (C) PCR confirmation of N19 library of n = 30 colonies selected at random. Presence of N19 library confirmed in 27 out of 30 colonies (90%). (D) DNA sequencing of positive colonies confirms N19 library produces unique randomized 19bp long sequences. (E) NCBI BLAST of clone #1 showing that sequences do not completely match coding genes

These data demonstrated that all there were no complete matches to protein coding genes. These results were expected given the plasmid design. Using a small transcript of 19 bases limited the likelihood that the transcript would be translated to a protein and increased the likelihood that the transcript would potentially function as a decoy. Together these data demonstrate that we designed a library capable of expressing upwards of $3x10^7$ unique single stranded noncoding RNA sequences that are 19bp in length.

2.2.2 Establishing BRAFi resistant cell lines using the N19 Library

The goal of this project is to elucidate the role of noncoding RNA in targeted therapy resistance in human melanomas. Therefore, we selected three common human melanoma cell lines to test our hypothesis. Mel888 was resected from a 26 year old female patient with metastatic melanoma. Mel624 was resected from the metastatic melanoma of a male patient of an unspecified age. Both tumor cell lines have the $BRAF^{V600E}$ mutation. That means both are expected to demonstrate sensitivity to BRAFi's like vemurafenib. Before treating the cells with the library, it was important to understand baseline sensitivity to vemurafenib at different doses. Figure 2.5 shows phase contrast imaging at 25X of the two melanoma cell lines treated with 3 different doses of vemurafenib dissolved into DMSO and added to DMEM cell culture media with 2% FBS and a 1% DMSO vehicle control added to DMEM cell culture media with 2% FBS over 5 days at 37ºC. After 5 days, the wells were washed 3 times with 500 µl of 1X PBS.

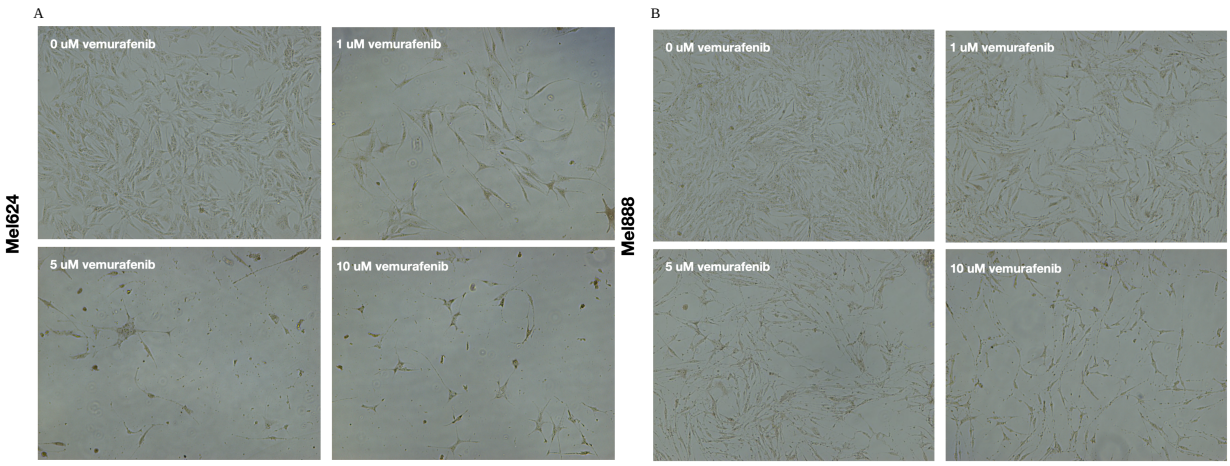

Figure 2.4. Testing sensitivity to BRAFi of two representative human melanoma lines
100x phase contrast imagine of (A) Mel624 cells and (B) Mel888 cells were plated at about 75% confluence in DMEM cell culture media with 2% FBS with 3 concentrations of vemurafenib (1μM, 5μM, 10μM) solubilized in DMSO with 10% DMSO vehicle control

The Mel624 cell line showed sensitivity to 5μM vemurafenib and the Mel888 cell line showed sensitivity around 10μM. As previously mentioned, we expected treatment with vemurafenib to induce cell death in both cell lines. We also expected for each cell line to have a slightly different sensitivity to vemurafenib as the cell lines are derived from two different patients. Moving forward with these two cell lines with their slightly different genetic backgrounds and sensitivities to vemurafenib increases the generalizability of our conclusions.

2.2.3 Comparing resistant cell lines to parental cell lines

After establishing the resistant cell lines (Figure 2.5), it was important to quantify just how much more resistant to treatment our experimental lines were than their parental counterparts.

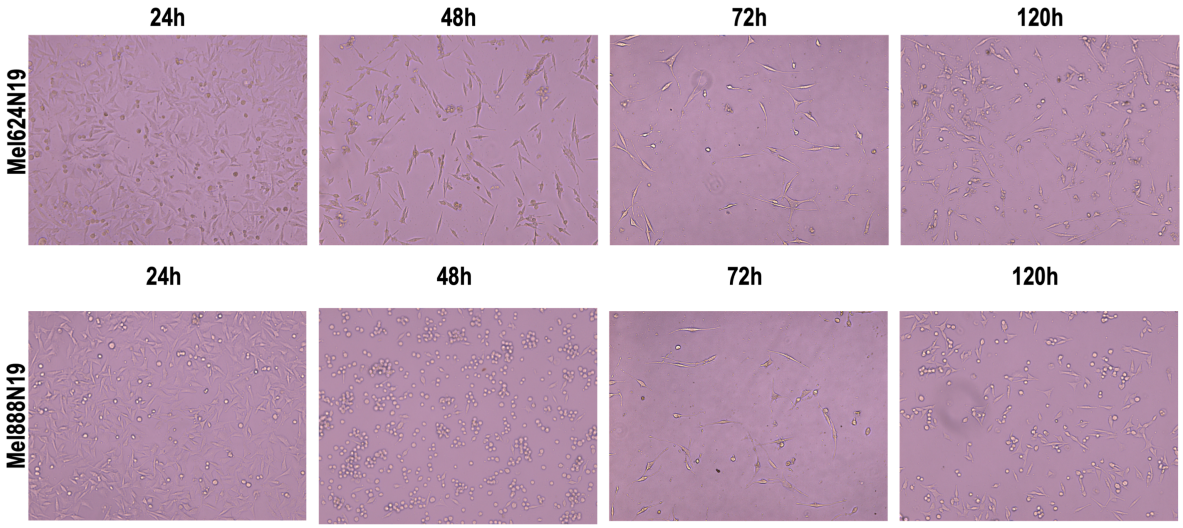

Figure 2.5. Establishing BRAFi resistant melanoma cell lines using the N19 RNA library
(Top) 100x phase contrast images of the Mel624 cell line and (Bottom) the Mel888 was stably infected with the packaged retroviruses containing the N19 RNA library and treated with 5μM vemurafenib over 5 days. The remaining cells at day 5 were expanded.

To start, we plated equal sub confluent numbers of the parental cell lines (Mel624 and Mel888) and their resistant counterparts (Mel624N19 and Mel888N19) on six well plates and treated them with three different doses of vemurafenib over 5 days. On day 5, we performed a crystal violet staining on each well to visualize living cells. We quantified those crystal violet results with an OD490 scan of the plates. Figure 2.6 shows those results.

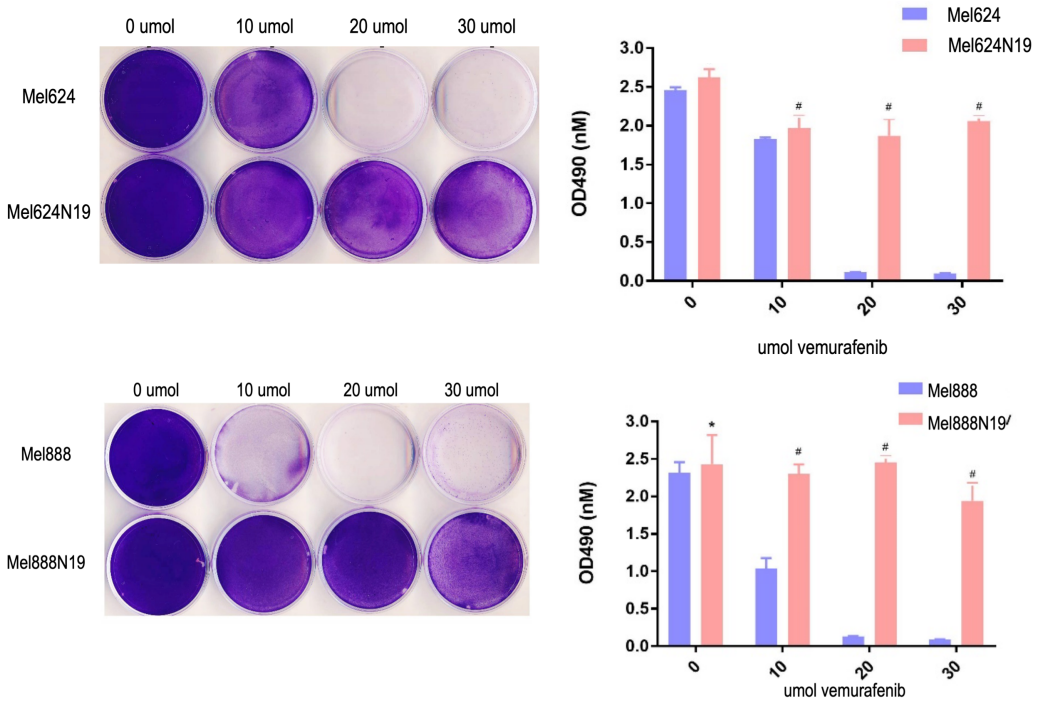

Figure 2.6. Testing BRAFi on parental cell lines and N19 resistant library lines
(Top) Mel624 cells and (Bottom) Mel888 cells were plated at about 75% confluence in DMEM cell culture media with 2% FBS and 3 different doses (10uM, 20uM, 30uM) vemurafenib solubilized in DMSO along with a DMSO control

From those results we concluded that Mel624N19 was more resistant than its parental cell line at two doses of vemurafenib (20 μM and 30 μM). Mel888N19 was more resistant at three different doses of vemurafenib (10 μM, 20 μM, and 30 μM). Given that our library contains a multitude of randomized 19mers we expected some variability between cell lines in this assay as well.

We also performed a scratch assay to provide a readout for cell migration following treatment with vemurafenib (Figure 2.7). Cells from parental lines (Mel624 and Mel888) and library lines (Mel624N19 and Mel888N19) were plated at about 100% confluence on 24 well plates in DMEM cell culture media with 2% FBS and 10% DMSO or 5 μM vemurafenib dissolved in 10% DMSO. A scratch was introduced to the middle of each well with an autoclaved p20 pipette tip. 72 hours later, both the parental cell lines and the library cell lines in the untreated condition demonstrated normal cell migration and a closed scratch. In the 5 μM condition, both the parental cell line and the library cell line showed a reduction in cell migration.

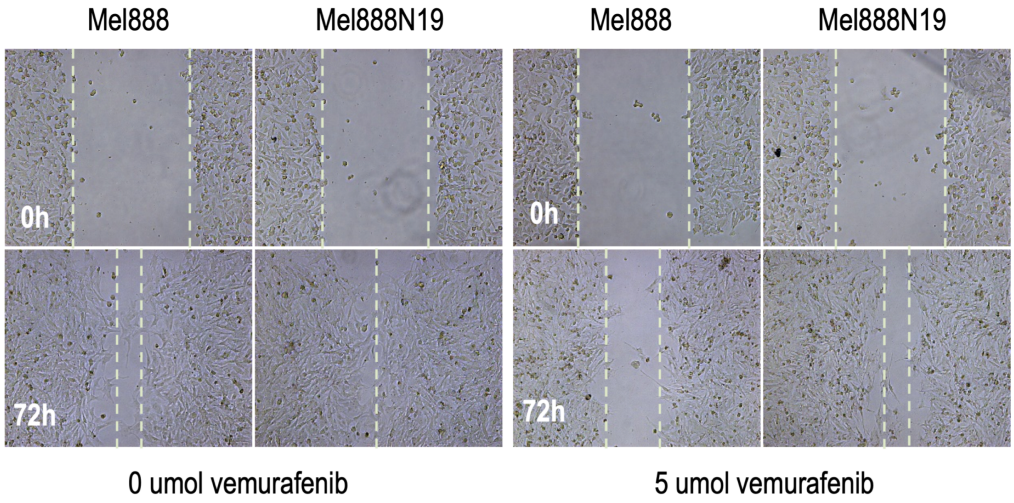

Figure 2.7. Scratch assay confirming N19 resistant library cell motility
(Left) 25x phase contrast imaging of Mel888 and Mel888N19 cells were plated at 100% confluence in DMEM cell culture media with 2% FBS with 10% DMSO vehicle control and a scratch was created in the middle of the well at 0h (top). At 72h (bottom) the scratch surface area was remeasured using ImageJ. (Right) 25x phase contrast imaging of Mel888 and Mel888N19 cells were plated at 100% confluence in DMEM cell culture media with 2% FBS with 5uM vemurafenib solubilized in DMSO (totaling 10%) and a scratch was created in the middle of the well at 0h. At 72h (bottom) the scratch surface area was remeasured using ImageJ.

Though this dose is below the lethal threshold shown in Figure 2.6, this result is expected. The hypothesis is that vemurafenib may simply slow proliferation at a sublethal dose without causing any major cell death. The library cells demonstrated significantly less sensitivity to the low dose of vemurafenib by closing the gap more than the parental cell line. This suggests that treatment with vemurafenib had a reduced impact on both cell proliferation and cell migration in the library cell lines.

Consistent with the literature, melanoma cell lines display a wide array of defects when it comes to cell cycle regulation[63]. In fact, combination therapy with CDK4/6 cell cycle inhibitors and BRAFi were once investigated as a possible combination therapy to overcome BRAFi resistance[12]. We treated parental cells (Mel888) and library cells (Mel888N19) with 10 μM of vemurafenib dissolved in 10% DMSO in DMEM cell culture media with 2% FBS. After 3 days of treatment, we assessed the cell cycle profile of both cell lines using flow cytometry (Figure 2.8).

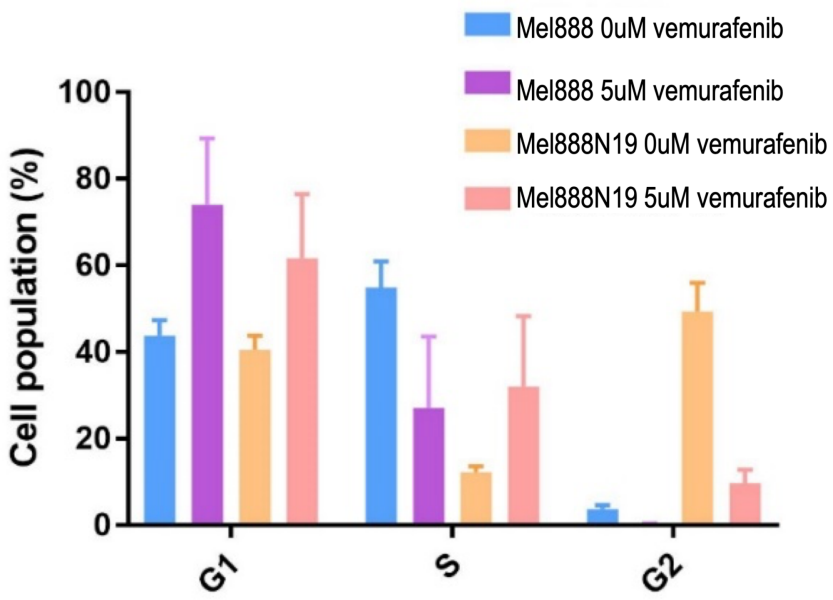

Figure 2.8. Cell cycle analysis of Mel888 and Mel888N19 cells with and without BRAFi
Mel888 and Mel888N19 cells were cultured in DMEM cell culture media with 2% FBS and 10% DMSO or 5μM vemurafenib solubilized in 10% DMSO for three days.

Most of the untreated parental cells were in S phase (about 56%) or G1 (about 40%). Introduction of the library appeared to cause a shift in cell cycle distribution toward G2. This might suggest that the library cells are more primed for proliferation which is consistent with the resistance phenotype. When treated with 10 μM vemurafenib, the parental line shifted drastically to G1 with almost 80% of cells being in that phase of the cell cycle. However, the library cell line displayed a less dramatic shift to G1 with some other portion of the shift being into S phase. There were still a significant number of library cells in G2 phase following treatment with vemurafenib. These data are consistent with the idea that sublethal doses of vemurafenib only slow proliferation of library cells. These results are also consistent with the fact that the resistance phenotype takes time to develop. Presumably, after 3 days the resistant cells would begin to proliferate at normal levels.

Since we observed that 3 days of treatment with vemurafenib was sufficient to induce changes in cell cycle, we next wanted a quantitative measure of cell viability at sublethal doses for the parental cell lines as well as the library cell lines. To answer this question, we treated both Mel888 and Mel888N19 with 4 doses of sublethal vemurafenib and measured cell viability with a colorimetric assay after 3 days (Figure 2.9).

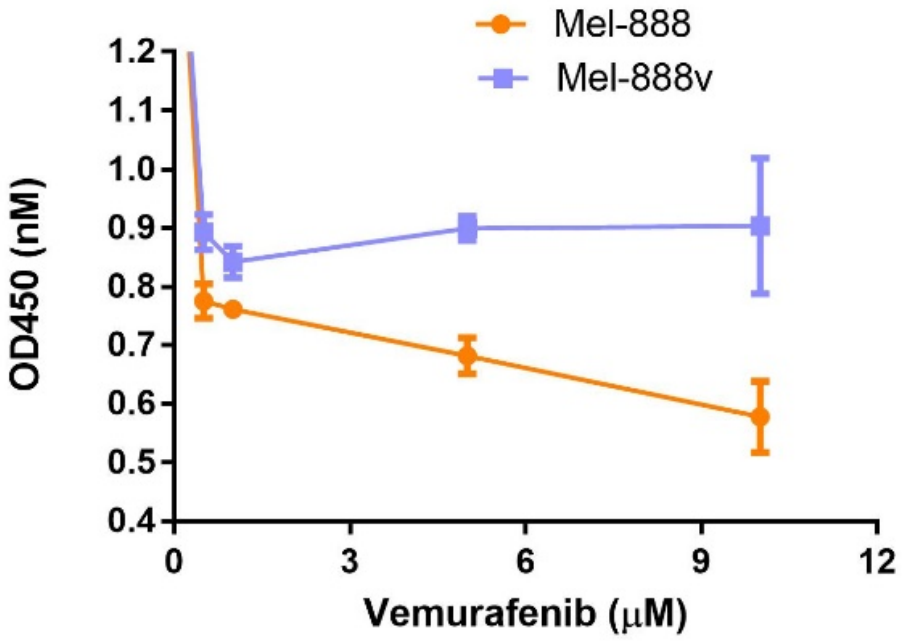

Figure 2.9. Comparing vemurafenib sensitivity between the parental Mel888 cell line and the Mel888N19 cell line

Both cell lines were treated with 4 different doses of vemurafenib (0μM, 1μM, 5μM, 10μM) and cell viability was measured using a colorimetric response.

Treatment with 0 μM and 1 μM of vemurafenib resulted in almost no cell death in both lines. After treatment with 5 μM, cell death significantly impacted the Mel888 cells while the Mel888N19 cells experienced a small increase in cell proliferation. When the dose of vemurafenib was doubled to 10 μM, the parental cell line Mel888 saw another significant decrease in cell viability. However, the population of the library cell line Mel888N19 remained stable. These data confirmed that the introduction of the library conferred resistance to treatment with vemurafenib even in a cell line that has a high susceptibility to treatment.

2.2.4 Verifying that the resistance phenotype is biologically relevant

As previously highlighted, the vemurafenib resistance phenotype emerges soon after treatment is initiated and it is driven by pharmacodynamics as well as coordinated expression of a vast number of genes. Because our library is synthetic and novel, it is unknown whether or not the resistance phenotype was biologically relevant. In order to answer that question, we separated resistance genes to analyze into three different categories: driver genes, epithelial to mesenchymal transition (EMT), and BRAF related genes. Driver genes are identified as such because of their ability to drive abnormal and uncontrolled cellular growth[64]. As previously mentioned, melanoma has one of highest somatic mutational burdens among solid malignancies[13]. We selected the following prominent melanoma driver genes for their ability to produce cell surface receptors that bind mitogens that induce downstream cell proliferation: EGFR (EGFR protein), FLT1 (VEGFR1 protein), and KDR (VEGFR2 protein). We selected MTOR (mTOR protein), AKT1 (AKT1 protein), and PTEN (PTEN protein) due to their roles in cell growth and proliferation signaling pathways. The EMT category was of interest because

EMT genes play important roles in all stages of cancer progression from initiation, primary tumor growth, invasion, dissemination, metastasis, and colonization to resistance to therapy[65,66]. Over-expression of the cytoskeletal protein VIM is associated with aggressive disease and worse outcomes in a wide range of cancers including melanoma[67]. FOXC2 is a transcription factor that when over-expressed it promotes melanoma outgrowth and regulation of genes associated with drug resistance[68]. SNAIL1 is a prominent inducer of EMT that strongly represses E-cadherin expression thereby conferring tumor cells with cancer stem cell like traits, drug resistance, tumor recurrence, and metastasis[69]. OCLN is a tight junction protein and MMP14 is an enzyme responsible for degrading extracellular collagen. TWIST is known to be over expressed in melanoma cell lines that have been cultured from invasive, pre-metastatic tumors associated with poor clinical prognosis[70]. The BRAF related genes are all significant components of the MAPK signaling pathway. Normally, HGF is not secreted by melanocytes[71]. However, in the case of melanoma, HGF and its receptor c-MET are both over expressed; resulting in autocrine signaling that activates cell growth and proliferation[71]. NRAS, BRAF, MEK1, MEK2, and RAF1 are all components of the MAPK signaling pathway that are dysregulated in treatment resistant melanoma. Relative mRNA expression levels for all of these biologically relevant proteins were measured after 5 days of treatment with 5 μM of vemurafenib. Figure 2.10 shows that relative mRNA expression levels were higher for each gene in the library cell lines.

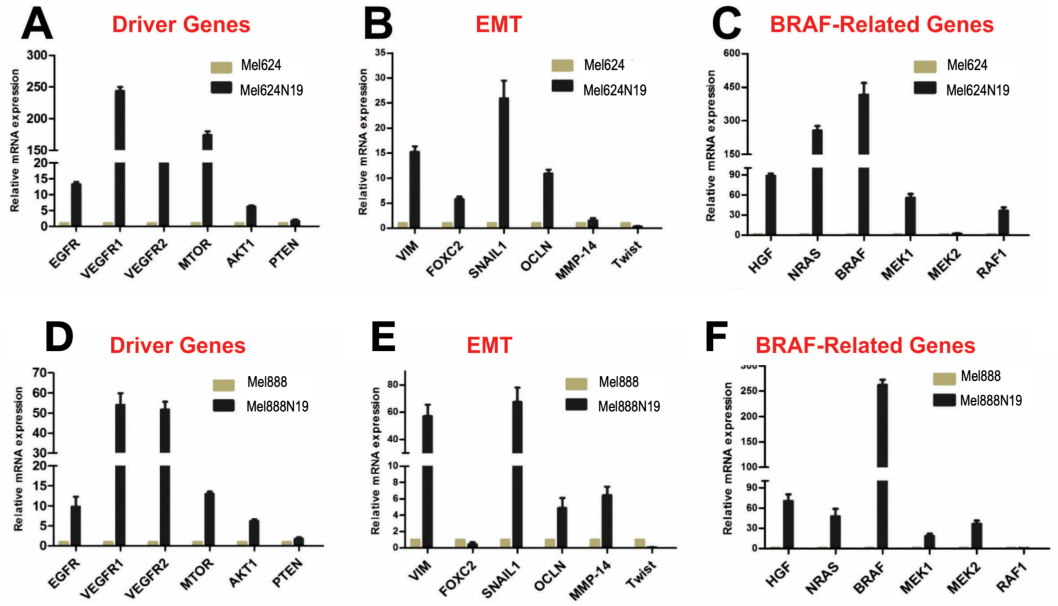

Figure 2.10. qPCR of canonical BRAFi driver genes, EMT genes, and BRAF related genes mRNA levels of proteins previously described in resistance literature were studied comparing the Mel888 parental cell line expression levels to the Mel888N19 resistant library cell line expression levels.

These data suggest that the resistance phenotype exhibited by the library cell lines is due to a gene expression profile that is consistent with preclinical and clinical data.

2.2.5 Individual enriched VRT sequences recapitulate resistance phenotype

In Chapter 1, we demonstrated that delivering the N19 library to parental cells meant delivering upwards of $3x10^7$ unique N19 noncoding transcripts to cell population. But, we are still uncertain as to which transcripts are responsible for the resistance phenotype. To answer that question, we completed nested PCR on the genomic DNA isolated from the library cell lines with the goal of DNA sequencing the 19mer from our plasmid. We identified the top 20 most enriched 19mer sequences in both library cell lines (Table 2.1).

Mel 888 N19

Average Raw Counts	% of total valid counts	N19mer Sequence
2628461.0	35.910	ACAAGTTAACGGACGCAAT
2131942.0	29.133	TATTGTTGTAGACGAAACT
144779.0	1.964	GGGAGCTCAGCTGTCCAGC
98247.5	1.332	GGGAAGTCAGATCGGTTCT
84395.5	1.143	CAATAGAGGGGTTAACCGG
83385.5	1.131	GCCTCGGAGATCGGCATAG
46155.0	0.625	ATATAAAATGGATGGCAAC
45970.0	0.623	TATACACCAGATACCAAGT
39946.0	0.542	ATCACTTGAACAACTACAC
37393.5	0.506	CGCACTGTGTTGGGTAAAT
37182.5	0.504	GGCGAGTAATCCTACGTGT
33518.5	0.457	CCAAGTTAACGGACGCAAT
31806.5	0.431	GCATATGAAGCGCCACGTT
30764.5	0.418	AAGGACAGCGAACTGAGTT
30424.0	0.415	TATTGTTGTAGACGAAACC
28595.5	0.388	AGAGACGAAGAGTGAGGCA
24354.0	0.329	CAGGTAGATGCACTGAAGA
23388.5	0.319	GCAAGTTAACGGACGCAAT
21632.0	0.295	TATTGTCGTAGACGAAACT
21335.0	0.291	ACGAGTTAACGGACGCAAT

Mel 624 N19

Average Raw Counts	% of total valid counts	N19mer Sequence
557051.0	11.064	TCGGCACTTTCTCGTTGGA
309658.0	6.150	CAGGCCCCTCTACTCTACC
252852.0	5.022	CCCGCCGCTCGTCCTCTTG
236310.0	4.694	CTTGCTCCGCGCAGGGCGC
186127.0	3.697	AAGTAGGTAAGCCCAATTT
179186.0	3.559	AGCATGTGATGTAGTGGAG
177363.0	3.523	CAAACCCCAAAACAGATCA
121947.0	2.422	GACTAATGTTCCATACTGA
108956.0	2.164	AATTGTAGTCGATACGTGG
81522.0	1.619	TACTAAGATGCGAATGCCA
77132.0	1.532	AGACACGAGTTATTCTGTG
51564.0	1.024	TTTGTTTAGAACAAGAGAA
46259.0	0.919	TCCCCCCGTCCCAGTCGGC
45415.0	0.902	GGTTGAACTAATGGTAGCA
39290.0	0.780	CGGTAAAAATTAAAAAGAT
37286.0	0.741	TGCAACTATAATACCAAGA
37212.0	0.739	CTAGTAAGAAAAACCATCG
33375.0	0.663	AGCTTAGCTGAAAAAATAG
33214.0	0.660	CATTCGATACATCAAAGTC
32313.0	0.642	GCCTCCAGGGTCGGATTCT

Table 2.1. Enriched 19mer sequences in the resistant cell population

The top 20 most enriched 19mer sequences in the (left) Mel888N19 resistant library cell line and the (right) Mel624N19 resistant library cell line

More than 65% of the enriched 19mers in the Mel888N19 library were from two transcripts. The enrichment profile of the Mel624N19 library cells was more evenly distributed with 9 transcripts showing more than 2% enrichment in the population. Moving forward with the 2% enrichment threshold, we identified 10 vemurafenib resistant transcripts (VRTs) across both cell lines to test their ability to confer resistance to treatment at several doses. Interestingly enough, the VRTs from the Mel624N19 line were almost unrepresented in the Mel888N19 enrichment profile and vice versa. Before testing the ability of each individual VRT to confer resistance, we verified that the enriched sequences served a regulatory function. Rarely did any of the top 1000 most enriched sequences map to coding genes. Only 0.1% of the enriched 19mers mapped to coding genes when no mismatches were accounted for (Figure 2.11).

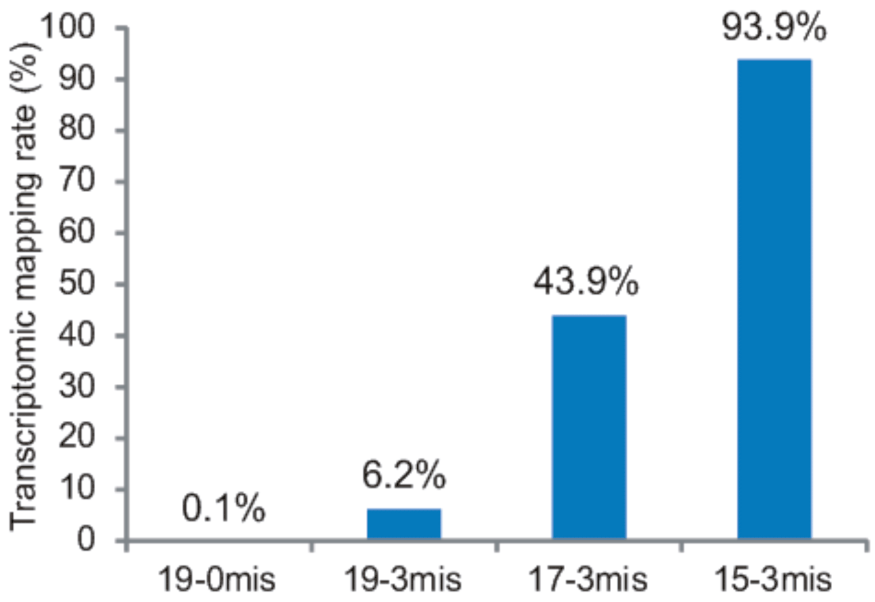

Figure 2.11. Transcriptomic mapping rate of library generated 19mers
Percentages of N19 generated 19mers that match to coding genes with (first column) no mismatches allowed, (second column) 3 mismatches allowed, (third column) 17 base pairs and 3 mismatches allowed, (fourth column) 15 base pairs and 3 mismatches allowed.

We repackaged each of the VRTs into different plasmids and used them to develop resistant cell lines using the same process mentioned in Section 2.2 (Figure 2.12).

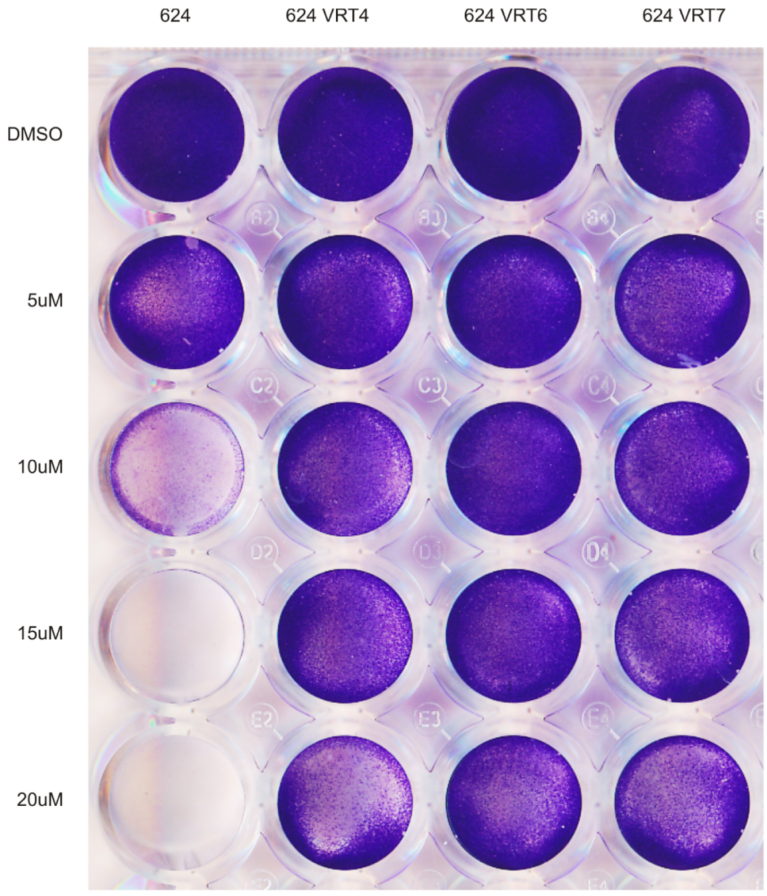

Figure 2.12. Individual VRTs confer resistance to vemurafenib treatment over several doses

Parental Mel624 cells and VRT cell lines Mel624VRT4, Mel624VRT6, and Mel624VRT7 were plated at 75% confluence and cultured in DMEM cell culture media with 2% FBS and 4 different doses (5μM, 10μM, 15μM, and 20μM) of vemurafenib solubilized in 10% DMSO and a vehicle control of 10% DMSO. After 3 days of culture, each well was stained with crystal violet staining.

What stood out about generating resistant lines from the individual VRTs is that they tended to show higher initial resistance to vemurafenib than the library lines. This meant that there was a decrease in cell death at 24h and 48h post treatment in the individual VRT cell lines than the library cell lines. After the resistant cell lines were established, we selected three VRT cell lines and compared their resistance to vemurafenib over several doses to their parental cell line using the same crystal violet staining from Section 2.3. Where the Mel624 parental cell line exhibited sensitivity to 10 μM of vemurafenib, Mel624VRT4, Mel624VRT6, and Mel624VRT7 cells exhibited resistance to treatment at 20 μM (Figure 2.12). These data suggested that enriched 19mers had the ability to confer resistance to vemurafenib.

It was unknown whether or not the VRTs enriched in Mel624N19 would confer resistance to vemurafenib in Mel888 cells. To address this, we used crystal violet staining to compare the resistance phenotype of VRTs 1 through 12 in Mel888 cells to both the parental cell line and the N19 library cell line (Figure 2.13).

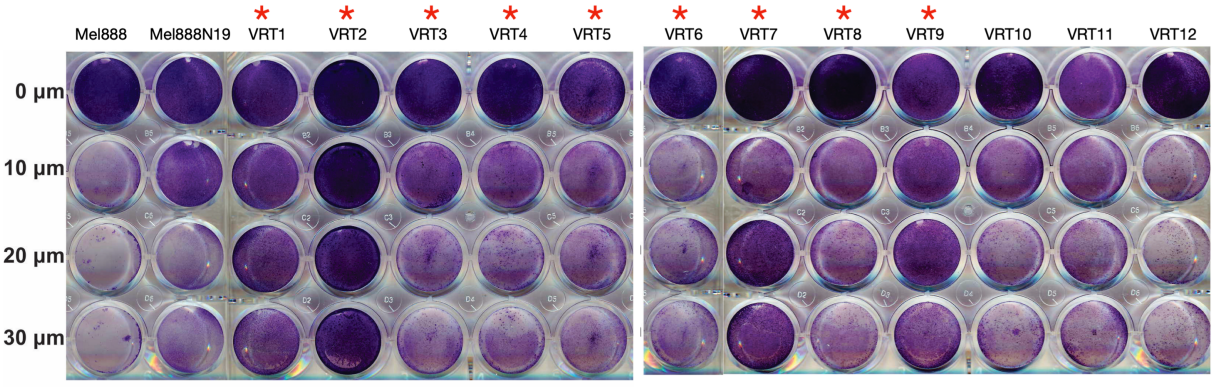

Figure 2.13. Individual VRTs confer resistance to vemurafenib treatment over several doses

Parental Mel624 cells and VRT cell lines Mel624VRT4, Mel624VRT6, and Mel624VRT7 were plated at 75% confluence and cultured in DMEM cell culture media with 2% FBS and 4 different doses (5µM, 10µM, 15µM, and 20µM) of vemurafenib solubilized in 10% DMSO and a vehicle control of 10% DMSO. After 3 days of culture, each well was stained with crystal violet staining.

Across the board, the VRT lines displayed resistance equal to or greater than the Mel888N19 library lines. These data—particularly the data from VRTs 1 through 9—suggest that the individual VRTs confer resistance to vemurafenib regardless of their cell line of origin.

2.2.6 Consensus VRT1000 sequences also recapitulate resistance phenotype

In the previous section we confirmed the ability of individual VRTs to confer resistance to vemurafenib regardless of their cell line of origin. What remained unknown is if there was any genetic similarities between the VRTs that might explain their resistance conferring abilities. To answer that question, we created a consensus motif out taking into account each of the top 1000 most enriched VRTs and their enrichment percentages (Figure 2.14).

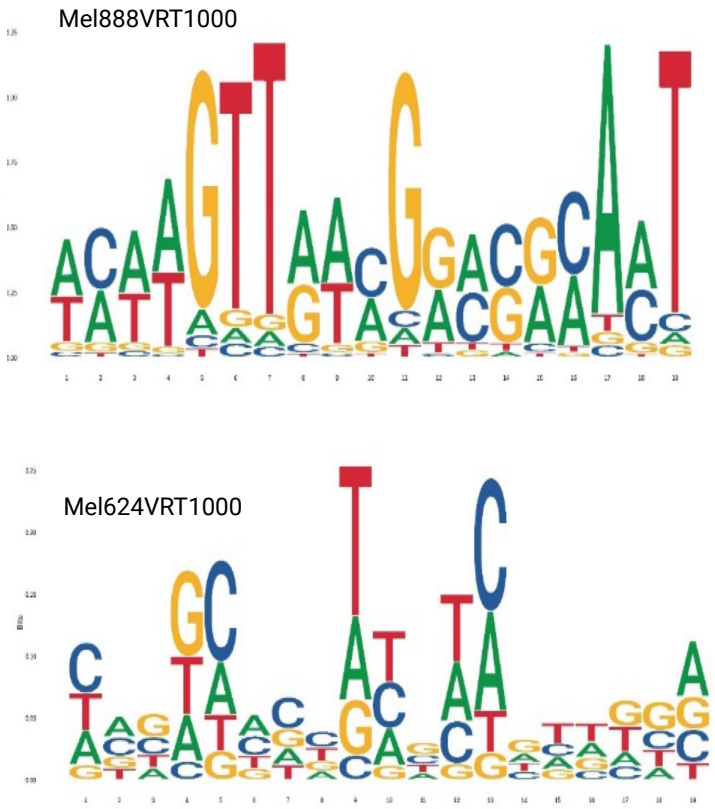

Figure 2.14. Consensus sequence for Mel888VRT100 and Mel624VRT1000
Consensus sequences of the top 1000 most enriched sequences taking their enrichment percentage into account for (top) Mel888 and (bottom) Mel624

This resulted in a Mel624VRT1000 sequence and a Mel888VRT1000 sequence. After generating plasmids for each of those two sequences, we established two resistant cell lines noticing the same pattern of higher initial resistance compared to their parental cell lines as mentioned in Section 2.5. Via crystal violet staining, both VRT1000 cell lines displayed higher resistance to vemurafenib than their respective parental cell lines (Figure 2.15).

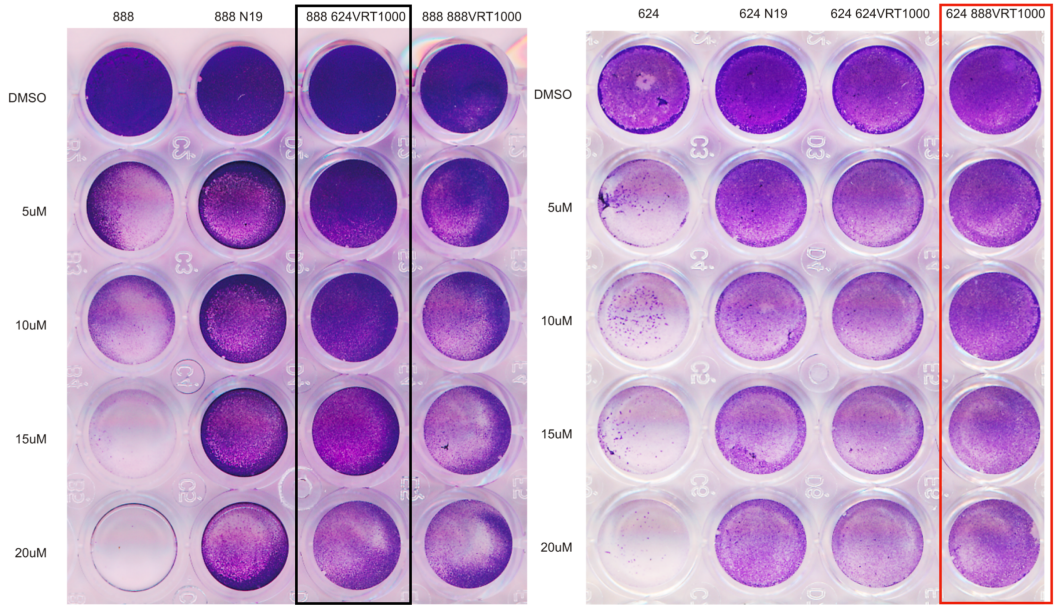

Figure 2.15. Individual VRTs confer resistance to vemurafenib treatment over several doses

Parental Mel624 cells and VRT cell lines Mel624VRT4, Mel624VRT6, and Mel624VRT7 were plated at 75% confluence and cultured in DMEM cell culture media with 2% FBS and 4 different doses (5μM, 10μM, 15μM, and 20μM) of vemurafenib solubilized in 10% DMSO and a vehicle control of 10% DMSO. After 3 days of culture, each well was stained with crystal violet staining.

These data suggest there is a structural quality to the 19mers that contributes to their ability to confer resistance. Interestingly enough, the VRT1000 established from the Mel624N19 enriched sequences also conferred resistance to vemurafenib in the Mel888 cell line and vice versa.

Chapter 3

Highlighting the significant changes to the transcriptome of resistant library cell populations in vitro

3.1 Introduction

The data from Chapter 2 suggested that introducing our N19 library and individual VRTs to parental cell lines resulted in a biologically relevant resistance phenotype. What remains unknown is the impact of delivering the library on gene expression. Drug resistance mechanisms are heterogenous from one melanoma to another. However, we demonstrated an ability to generate resistance in two different cell lines by delivering our N19 library, VRTs, and VRT1000s. This is especially important given the fact that one group showed that in response to BRAFi treatment changes to the transcriptome was cell line specific[72].

The role of noncoding RNA in melanoma resistance to BRAFi has been explored, but the mechanism is unclear. MITF is known to activate the expression of almost 100 genes in melanocytes; particularly genes related to differentiation, proliferation, migration, and senescence[73]. So, its direct post-transcriptional regulation is an important factor in understanding the resistance phenotype. The MITF transcript is under the control of noncoding RNAs[74]. This demonstrates that targeting noncoding RNAs is a viable option. The benefit of our library is that we get to target several pathways at once. In this chapter we leveraged our library system to investigate how noncoding RNA species might connect those resistance pathways to one another. These finding have implications as biomarkers as well. It would be extremely beneficial if

clinicians were able to profile the transcriptome of a tumor to predict its relevant resistance pathways.

The data from Chapter 2 suggested that introducing our N19 library and individual VRTs to parental cell lines resulted in a biologically relevant resistance phenotype. We hypothesize that result is due to our library and VRTs acting as sponges for other noncoding RNA molecules; thus altering the transcriptome.

3.2 Results

3.2.1 Heat maps highlight patterns of differential gene expression between parental cell lines and library cell lines

We completed RNA sequencing on both parental lines and resistant library lines with both the N19 library and VRT1000 consensus sequences after treatment with 5uM vemurafenib or DMSO vehicle control. We observed that the addition of vemurafenib to the parental lines did not result in an extreme change in gene expression in the Mel888 cell lines (Figure 3.1).

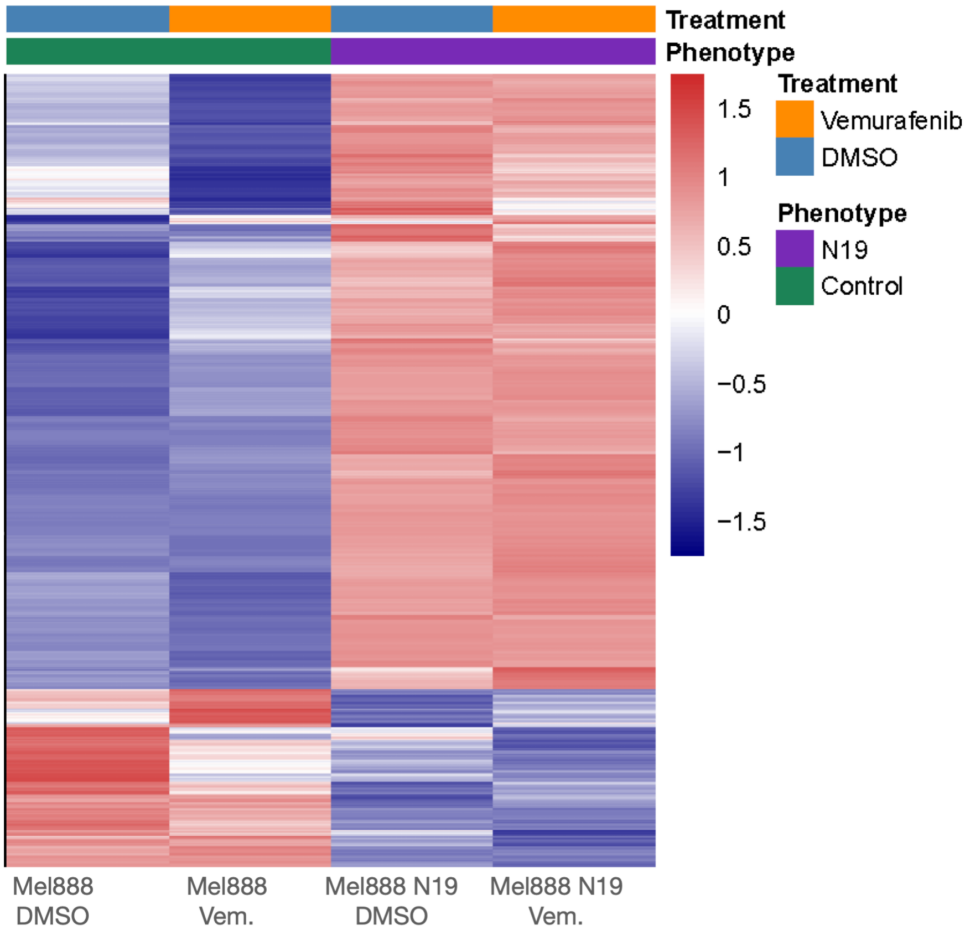

Figure 3.1. Transcriptomic profile changes after the administration of BRAFi
Heat map showing the transcriptomic profile of Mel888 parental cells and Mel888N19 resistant library cells after being treated with 5 μM vemurafenib (columns 2 and 4) and DMSO vehicle control (columns 1 and 3)

The noticeable global changes are likely responsible for the resistance phenotype. Though the overall treatment dose was sublethal, some marginal cell death is expected. So, some of the changes in gene expression could potentially be attributed to apoptosis. Introduction of the N19 library to the Mel888 cell line resulted in a noticeable change in global gene expression patterns regardless with or without drug treatment. This result was expected because we hypothesize that the library changes the noncoding RNA landscape in a way that biases molecules that contribute to the resistance phenotype. What is striking is the fact that the global gene expression profile appeared to be completely different from the parental cell lines regardless of treatment. We suspect that introduction of the library alone results in a change in the genetic landscape that lends itself to a resistance phenotype. We did observe slight differences in the global gene expression profile in library lines with the addition of vemurafenib. We suspect that those changes might be potentially related to novel resistance pathways.

Interestingly we observed a more drastic change in gene expression profiles between treated and untreated cells from the Mel624 line (Figure 3.2).

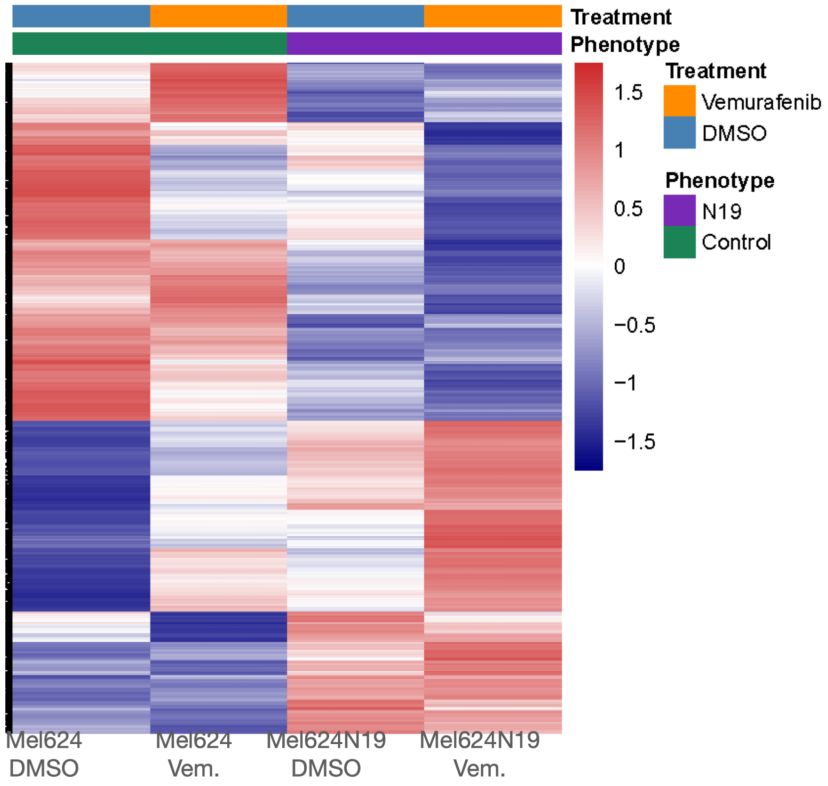

Figure 3.2. Transcriptomic profile changes after the administration of BRAFi
Heat map showing the transcriptomic profile of Mel624 parental cells and Mel624N19 resistant library cells after being treated with 5 µM vemurafenib (columns 2 and 4) and DMSO vehicle control (columns 1 and 3)

The result gives insight into why it was important for us to test our system in two different cel lines. As previously mentioned, the two different cell lines used in this project could be taken as two different patients with two different responses to treatment. Even more interesting is that introduction of the N19 library resulted in a more consistent gene expression profile between the treated cells and the untreated cells. However, the highly expressed genes were even more expressed and the lowly expressed genes were even less expressed when the library cells were treated with 5μM of vemurafenib. The next question to interrogate how introducing the VRT1000 consensus sequences might impact gene expression.

Introducing the VRT1000 consensus sequence into the Mel624 cell line resulted in a similar global gene expression shift as seen in Figure 3.3.

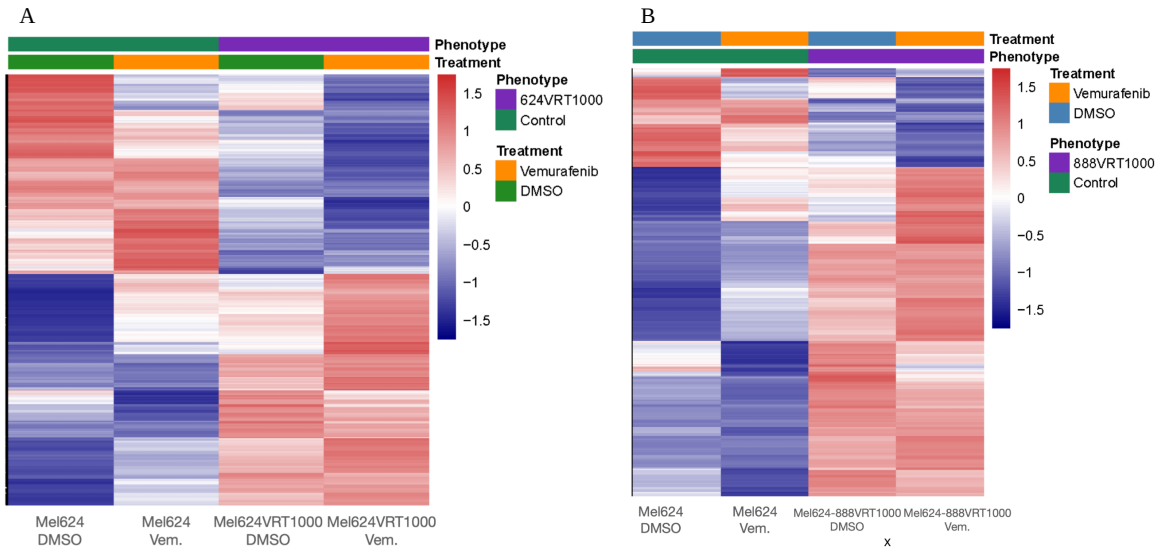

Figure 3.3. VRT1000 resistant cell lines recapitulate transcriptomic expression profiles of resistant N19 library lines

Heat map showing the transcriptomic profile of (A) Mel624 parental cells and Mel624VRT1000 resistant consensus sequence library cells after being treated with 5 µM vemurafenib (columns 2 and 4) and DMSO vehicle control (columns 1 and 3)

(B) Heat map showing the transcriptomic profile of (A) Mel624 parental cells and Mel624-888VRT1000 resistant consensus sequence library cells after being treated with 5 µM vemurafenib (columns 2 and 4) and DMSO vehicle control (columns 1 and 3)

This result suggests there is a structural element to the resistance phenotype generated by the N19 library. To demonstrate that this phenomenon is not limited to a particular cell line, we completed the same gene expression profile analysis after introducing the Mel888 consensus sequence into the Mel624 cell line as shown in **Figure XX**. Not only did the consensus sequence from the Mel888 cell line confer resistance to vemurafenib in the Mel624 cell line, but it also demonstrated a similar gene expression profile to the Mel624N19 library. Together these data suggest that the resistance phenotype generated by the library might be structural in nature.

3.2.2 Comparing gene expression profiles of different resistant cell lines sheds light on potential signaling pathways that explain differences in patient response

In order to more quantitatively analyze the difference in gene expression between the parental cell lines and the library cell lines, we used bioinformatic techniques. This allowed us to have a better understanding of just how many genes were differentially expressed between cell and library types.

In the previous section, we concluded that the N19 libraries confer resistance in some part due to their molecular structure. When comparing gene expression profiles of Mel888N19 versus Mel888VRT1000, we noticed that overall the N19 library induced unique up regulation of a total of 1340 identifiable genes and a unique down regulation of 311 genes as compared to the Mel888VRT1000 being responsible for an up regulation of 219 genes and a down regulation of 102 genes (Figure 3.4). Given the Mel888N19 library is more robust, we expected more genes to be impacted.

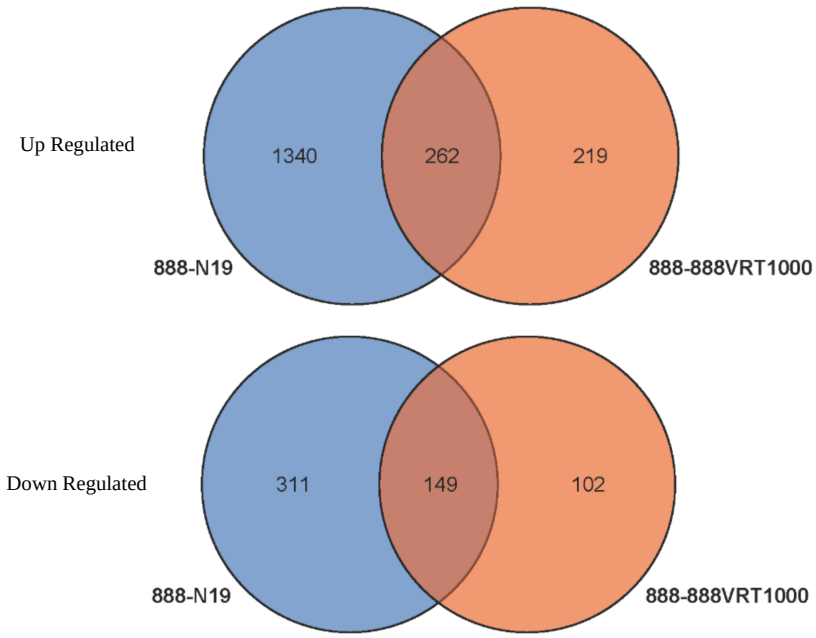

Figure 3.4. Up regulated and down regulated genes between library cell line and consensus VRT1000 cell line

Venn diagrams showing the number of genes (top) up regulated and (bottom) down regulated between the Mel888N19 (blue) resistant library cell line and the Mel888VRT1000 (red) resistant cell line

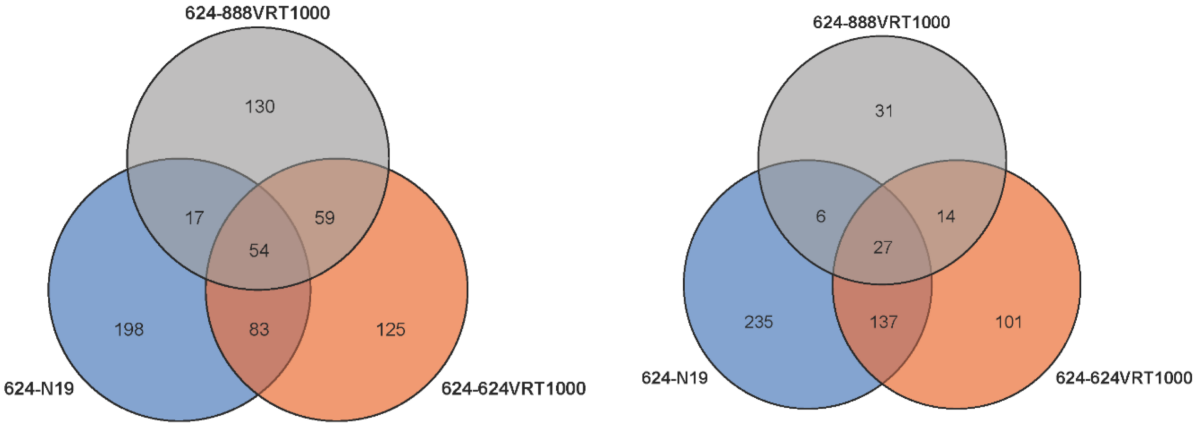

Figure 3.5. Up regulated and down regulated genes in library cell line and two consensus VRT1000 cell lines

Venn diagrams showing the number of (left) up regulated genes and (right) down regulated genes amongst the Mel624N19 (blue), Mel624-624VRT1000 (red), and Mel624-888VRT1000 (grey)

However, the VRT1000 consensus sequence was able to both up regulate and down regulate a significant number of genes on its own. The overlap of genes impacted by both the N19 library and the VRT1000 library might suggest that a single noncoding transcript is capable of a massive amount of gene regulation. This result is expected because noncoding RNA molecules have an extremely wide mechanism of action that does not require much specificity.

This pattern continued when comparing Mel624N19, Mel624-624VRT1000, and Mel624-888VRT1000 (Figure 3.5). There were a total of 71 shared up regulated genes and 33 down regulated genes between the Mel624N19 and the Mel624-888VRT1000 cell lines. This result indicated that the impact of noncoding library is not specific to a particular cell line. The resistant phenotypes can be generated by somewhat different genetic responses, but the drug stimulus is still the same.

3.2.3 KEGG plot highlights other relevant signaling pathways implicated in the resistance phenotype

In the previous section, we highlighted the number of genes with differential expression due to the various forms of the resistant library. The next question was to identify patterns in the types of pathways that were enriched in the resistant cell populations. To answer that question, we used bioinformatic techniques to generate a KEGG plot on the Mel888N19 library cells (Figure 3.6).

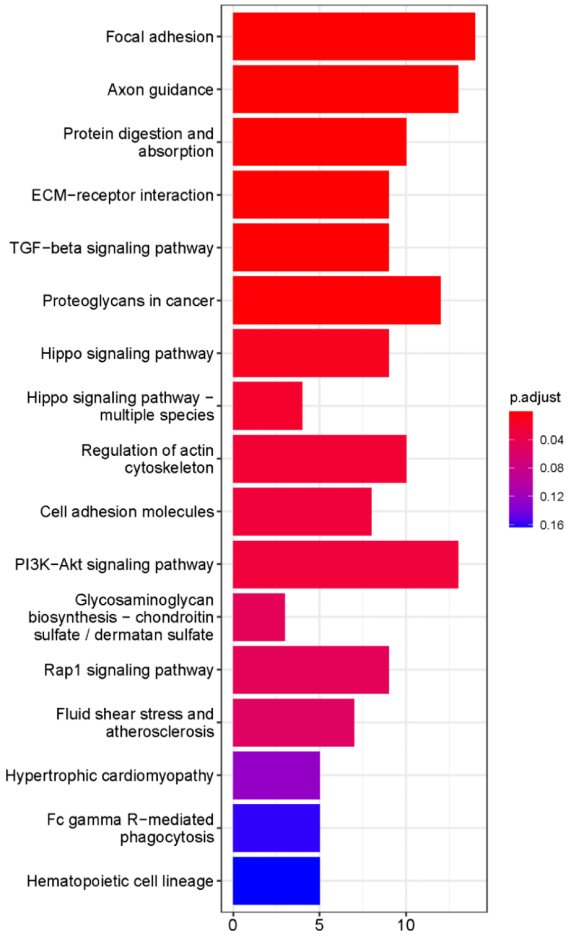

Figure 3.6. KEGG plot of genes involved in resistance phenotype

The genes fell into two major categories: cell morphology/EMT and growth and proliferation pathways. The cell morphology and EMT genes were involved in the following: focal adhesion, axon guidance, ECM receptor interaction, the TGF-β signaling pathway, and proteoglycans in cancer. We expect the resistance phenotype to involve cell morphology genes/ pathways. Changes in these genes allow the cells to ignore extracellular signaling to grow and proliferate. Additionally, changes in genes that regulate polarity are likely involved in both EMT and metastasis. The TGF-β signaling pathway is more difficult to pin down. In the early stages of cancer it is a known tumor suppressor. However, in late stage disease the pathway is associated with increased rates of metastasis. Upregulation of the TGF-β pathway is associated with increased resistance to BRAFi[75]. One of the several possible mechanisms of action is due to the fact that up regulation of TGF-β signaling induced activation of MEK and ERK; allowing for escape from BRAFi treatment[76]. Proteoglycans are involved in everything from cancer cell proliferation, to angiogenesis, to EMT and invasion. They are known to influence proliferation by interacting with external growth factors either via their protein cores or their associated glycosaminoglycans (GAGs)[77]. One proteoglycan in particular, CSPG4, has the ability to potentiate MAPK signaling[78]. As far as angiogenesis is concerned, elevated levels of the proteoglycan, biglycan, are associated with higher tumor associated blood vessel density[79]. The proteoglycan betaglycan is a co-receptor of TGF-β and is linked to EMT and invasion[80]. One of the more canonical growth and proliferation pathways associated with Mel888N19 resistance was the hippo signaling pathway. This result was expected given that increased expression of the microRNA miR-550a-3-5p is associated with increased vemurafenib sensitivity in resistant melanoma cells via YAP inhibition[81]. As previously mentioned, the PI3K-Akt signaling pathway

is an alternative growth and proliferation pathway used by BRAFi resistant melanoma cells. This pathway is also implicated in both the EMT and metabolism categories.

3.2.4 Volcano plots show individual genes

In the previous section, complex signaling pathways and gene expression processes were highlighted. In order to investigate the differential expression of particular genes we created a heat map showing the top 28 differentially expressed genes across all of the parental and library cell lines. The A2M gene was down regulated in almost all of the library lines. One group explained significantly low rates of cancer in naked mole-rats due to high expression of A2M[82]. This is because A2M inhibits the tumorigenic PI3K-Akt pathway. PAK1 is also universally up regulated in the library lines. PAK1 is often up regulated in cancer cell lines and it activates MAPK signaling which would be helpful in a resistance phenotype[83]. Volcano plots comparing parental Mel888 gene expression to Mel888N19 and Mel888VRT1000 gene expression highlight the same patterns (Figure 3.7).

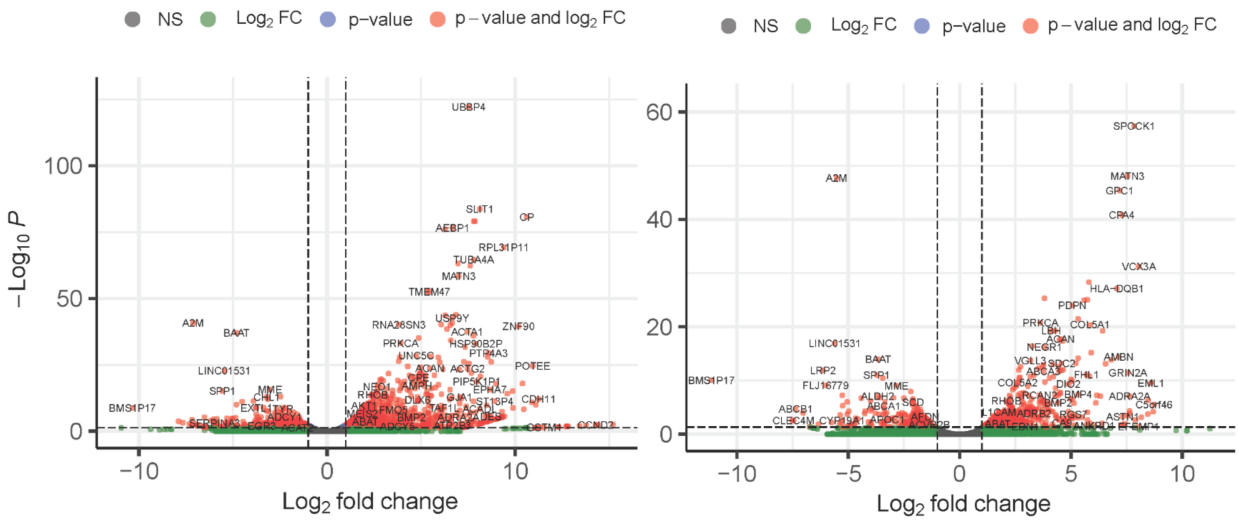

Figure 3.7. Individual VRTs confer resistance to vemurafenib treatment over several doses

Parental Mel624 cells and VRT cell lines Mel624VRT4, Mel624VRT6, and Mel624VRT7 were plated at 75% confluence and cultured in DMEM cell culture media with 2% FBS and 4 different doses (5μM, 10μM, 15μM, and 20μM) of vemurafenib solubilized in 10% DMSO and a vehicle control of 10% DMSO. After 3 days of culture, each well was stained with crystal violet staining.

The difference in up regulated genes between the Mel888N19 and the Mel888VRT1000 cell lines can be explained by the fact that the N19 library is more robust while the VRT1000 library depends on structural components for its impact.

Chapter 4

Investigating the impact of the regulatory RNA library, VRTs, and VRT1000s on the exomic DNA of resistant cell populations

4.1 Introduction

In Chapter 3 we verified differential gene expression patterns between our vemurafenib resistant library cell lines and the parental cell lines. As previously mentioned, melanomas tend to have high mutational burdens as far as solid tumors are concerned. An important next step to consider was whether or not delivering our library resulted in the passive enrichment or depletion of upstream single nucleotide variants (SNVs) in the cell population.

4.2 Results

4.2.1 Whole exomic sequencing reveals SNV changes in library cell lines

In Chapter 2 we demonstrated that our library likely has a regulatory function. In Chapter 3 we learned that our library impacts the transcriptome. So the next step is to determine whether or not introduction of our library impacts the genome of resistant cells. To answer this question, we submitted stably resistant library cells and parental cells for whole exomic sequencing. In Figure 4.1 the Circa map for the >50% threshold shows that there are loci throughout the genome with SNVs due to the introduction of the library.

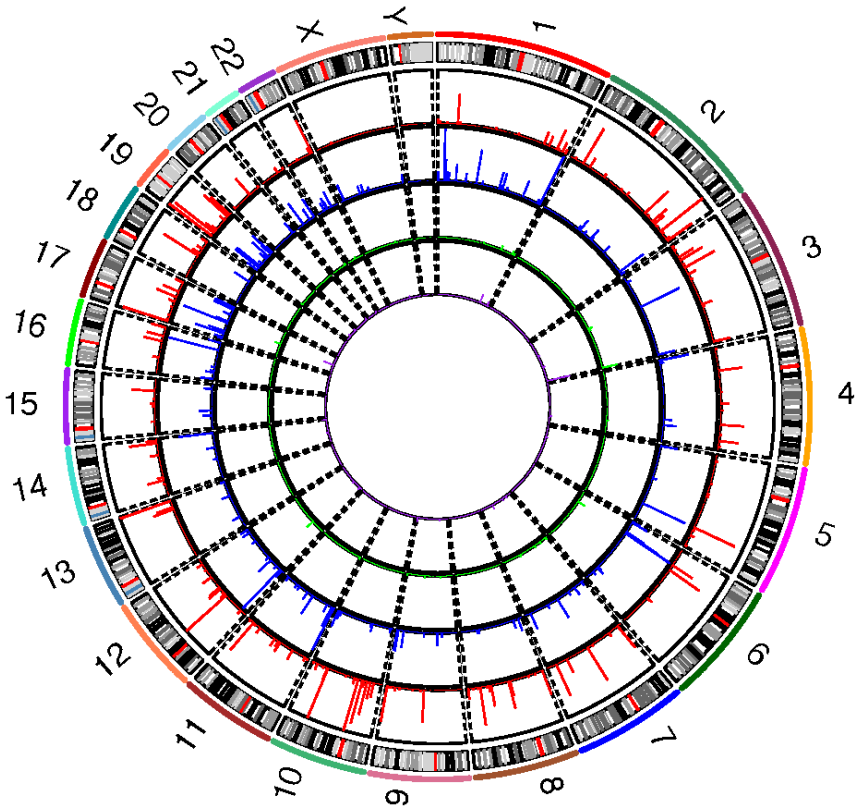

Figure 4.1. Circa map showing SNV changes >50%
(Red) Mel624N19, (Blue) Mel888N19, (Green) Mel888VRT1, (Purple) Mel888VRT10

There tend to be more SNVs in the larger N19 libraries in both cell types as compared to the individual VRTs. That result is expected given that the N19 libraries contain more resistance generating regulatory transcripts than the individual VRTs. Though there is some overlap in loci with SNVs between the Mel624N19 library line and the Mel888N19 library line, there are differences as well. This result is consistent with the rationale that two patients with BRAFi resistant melanoma can have tumors with different genetic profiles. When the threshold for SNV differences is lowered to >25%, the patterns are much easier to visualize. In Figure 4.2, we see the overlap in SNVs introduced by the VRT1 with VRT10.

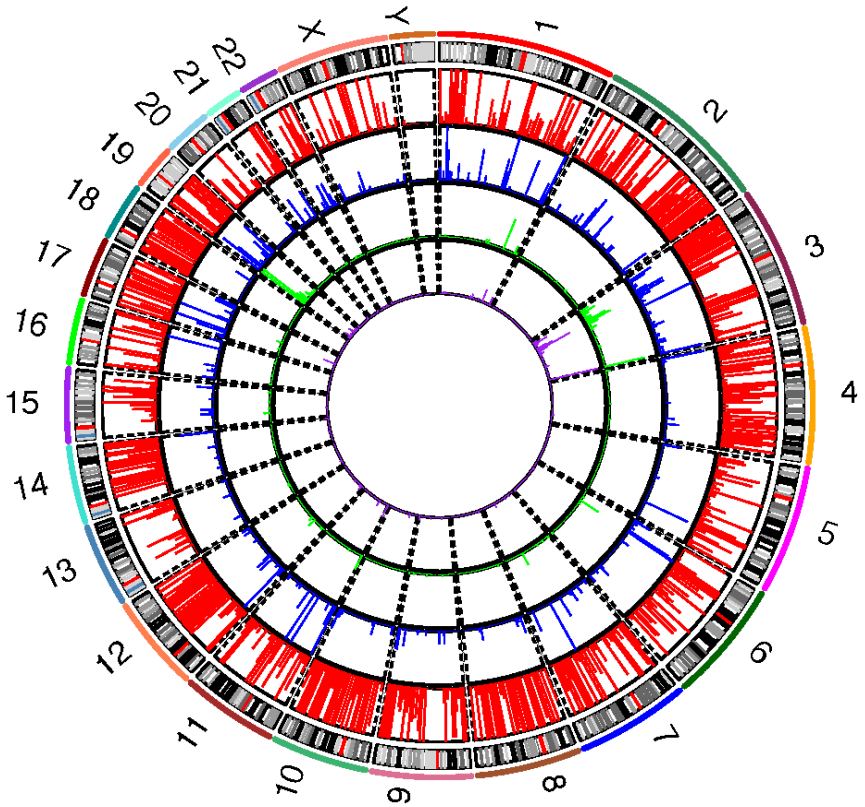

Figure 4.2. Circa map showing SNV changes >25%
(Red) Mel624N19, (Blue) Mel888N19, (Green) Mel888VRT1, (Purple) Mel888VRT10

It is worth noting that VRT1 was initially more enriched in the Mel624N19 library and that VRT10 was initially more enriched in the Mel888N19 line. The imperfections in the overlap may suggest that individual VRTs can confer resistance by targeting central similar pathways while also targeting unique complementary ones.

4.2.2 SNV frequency alteration profiles differ between the two library lines

The Circa maps from the previous section pinpoint the loci where the SNVs are found. What remains a question is how much above threshold are the changes in SNV frequency. Figure 4.3 shows that the SNVs found in Mel624 tend to be under represented in Mel624N19.

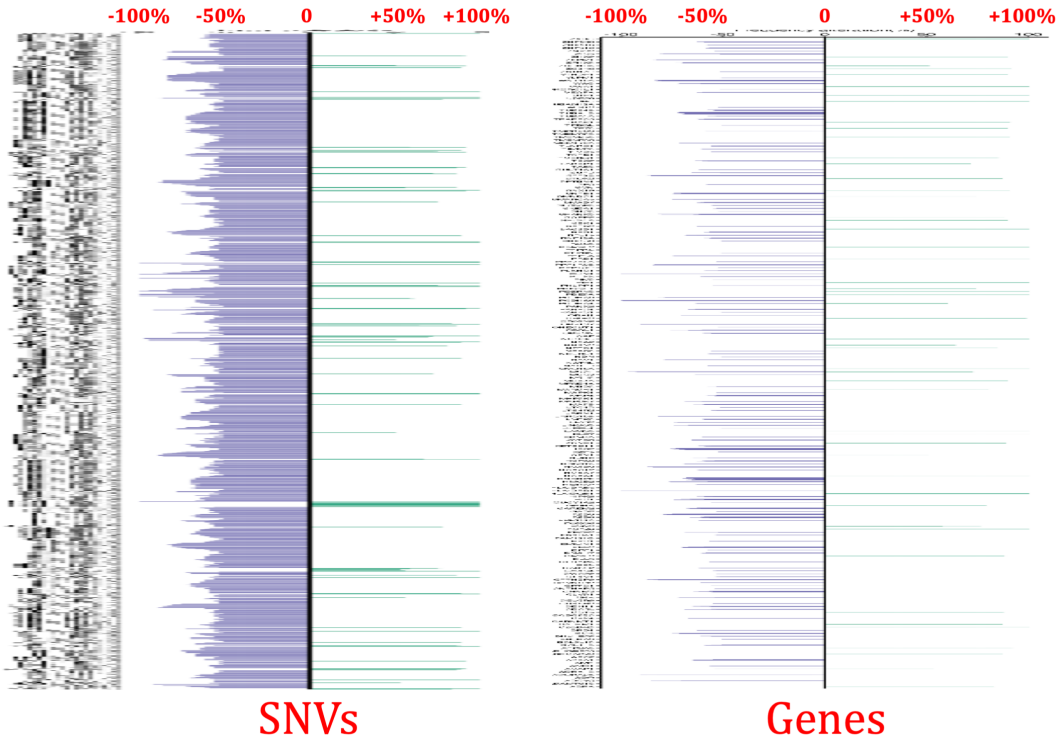

Figure 4.3. SNV changes >50% with associated genes (Mel624)

Several SNVs can be linked to a particular gene. Interestingly, introducing the library to Mel888 cells had the opposite effect. The SNVs found in Mel888N19 were in relatively low abundance in the Mel888 cell line as shown in Figure 4.4.

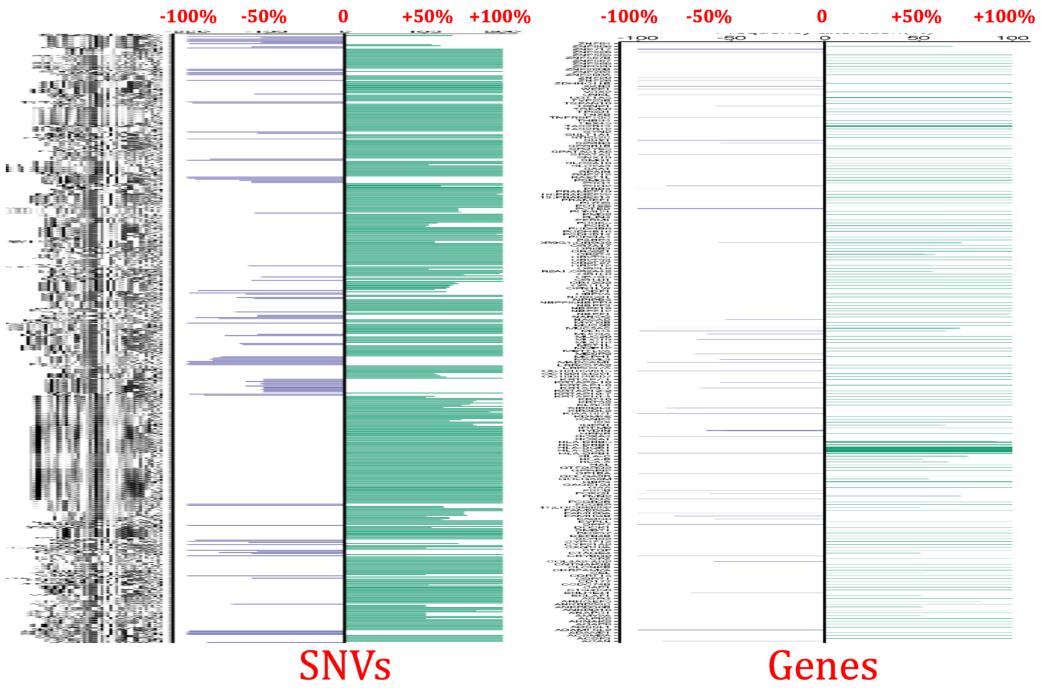

Figure 4.4. SNV changes >50% with associated genes

The Venn diagram in Figure 4.5 shows that significantly more genes in Mel624N19 were associated with SNV frequency alteration >50%.

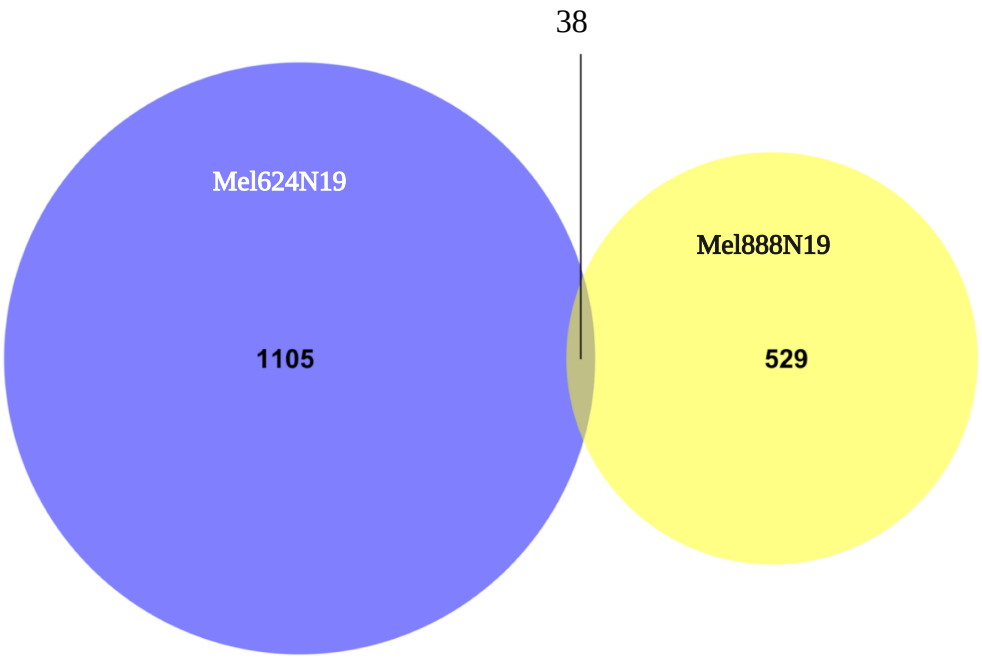

Figure 4.5. SNV changes >50% with associated genes (Mel624 v Mel888)
(Red) Mel624N19, (Blue) Mel888N19, (Green) Mel888VRT1, (Purple) Mel888VRT10

However, there were 38 genes shared between the two library cell lines with SNV frequency alteration >50%. These data are consistent with the rationale that certain genetic alterations are necessary to confer resistance and that many other complementary genes are involved.

4.2.3 Exonic function analysis of SNVs

We analyzed changes in the genetic code between the parental cell line Mel888 and the resistant library line Mel888-VRT1 (Table 4.1).

Gene name	ID	CHROM	POS	REF	ALT	Func	Exonic Func	Ratio change
XPC	rs2229089	3	14214524	G	A	exonic	missense SNV	26.55
SETD2	rs6767907	3	47162661	A	G	exonic	synonymous SNV	22.52
PBRM1	rs34341044	3	52637631	T	C	exonic	synonymous SNV	22.39
ABCC4	rs1751034	13	95714976	C	T	exonic	synonymous SNV	19.74
CIC	rs1052023	19	42799049	C	T	exonic	synonymous SNV	19.23
FLT1	rs2296189	13	28893642	A	G	exonic	synonymous SNV	16.37
SETD2	rs6767907	3	47162661	A	G	exonic	synonymous SNV	16.32
BRCA2	rs144848	13	32906729	A	C	exonic	missense SNV	16.20
IRS2	rs4773092	13	110435953	A	G	exonic	synonymous SNV	15.38
FLT1	rs2296189	13	28893642	A	G	exonic	synonymous SNV	15.32
GATA2	rs1573858	3	128205860	G	C	exonic	synonymous SNV	15.00
BCL10	rs11576939	1	85742012	G	C	exonic	synonymous SNV	-15.05
PBRM1	rs17264436	3	52610651	T	A	exonic	synonymous SNV	-15.11
ERCC1	rs11615	19	45923653	A	G	exonic	synonymous SNV	-15.21
IRS2	rs12853546	13	110435914	G	A	exonic	synonymous SNV	-15.95
XRCC1	rs915927	19	44057227	T	C	exonic	synonymous SNV	-16.00
CYP2A6	rs1137115	19	41356281	T	C	exonic	synonymous SNV	-16.38
WT1	rs2234582	11	32456694	C	A	exonic	synonymous SNV	-16.50
ERCC5	rs1047768	13	103504517	T	C	exonic	synonymous SNV	-17.28
ERCC2	rs1052555	19	45855524	G	A	exonic	synonymous SNV	-17.52
PBRM1	rs3755806	3	52643685	T	C	exonic	synonymous SNV	-17.53
CYP2A6	rs1137115	19	41356281	T	C	exonic	synonymous SNV	-17.76
FOXL2	rs750300712	3	138664931	G	C	exonic	missense SNV	-18.03
ERCC2	rs238406	19	45868309	T	G	exonic	synonymous SNV	-18.55
CIC	rs10410185	19	42795554	T	C	exonic	synonymous SNV	-19.30
CARD11	rs1621509	7	2969680	G	A	exonic	synonymous SNV	-19.49
CYP2B6	rs35303484	19	41497346	A	G	exonic	missense SNV	-20.40
ALK	rs4358080	2	30143499	G	C	exonic	synonymous SNV	-20.45
XRCC1	rs915927	19	44057227	T	C	exonic	synonymous SNV	-20.68
PBRM1	rs17264436	3	52610651	T	A	exonic	synonymous SNV	-21.10
ERCC1	rs11615	19	45923653	A	G	exonic	synonymous SNV	-22.27
CIC	rs10410185	19	42795554	T	C	exonic	synonymous SNV	-22.97
PBRM1	rs2251219	3	52584787	T	C	exonic	synonymous SNV	-23.04
MST1R	rs1062633	3	49924940	T	C	exonic	missense SNV	-24.43
PBRM1	rs3755806	3	52643685	T	C	exonic	synonymous SNV	-24.88
XRCC1	rs915927	19	44057227	T	C	exonic	synonymous SNV	-27.36

Table 4.1. Types of SNV changes >50% with associated genes

Consistent with the idea that most mutations in melanoma are passenger mutations, the SNVs associated with library cell lines tended most often to be synonymous mutations. Even though these mutations result in the same amino acids, many of them could be found in genes associated with the resistance phenotype. One group found that a mutation in CIC was associated with acquired resistance to BRAF-MEK inhibition in multiple myeloma[84]. Though rare, familial melanoma is linked to germ line mutations in BRCA2[85]. Loss of function mutations in PBRM1 are associated with worse clinical outcomes in patients with a variety of cancers treated with immunotherapy[86]. Previous studies indicate that each of these genes requires a missense mutation that completely alters the function of the translated protein. However, our data indicate that these genes were associated with synonymous mutations. This might suggest some sort of epigenetic cataloguing of passenger genes. One group hypothesized that this may be done by altering the ability of miRNAs to bind the 3'UTR, coding sequence, or 5' UTR of mRNAs[87]. This impacts transcript stability and we hypothesize that protein expression in resistant library cells would be compromised as a result.

4.2.4 Differentially expressed genes linked to SNV frequency alteration

Combining our RNAseq data and our whole exomic sequencing data, we generated maps of differentially expressed genes and their associated synonymous SNVs. Figure 4.6 shows two genes in particular.

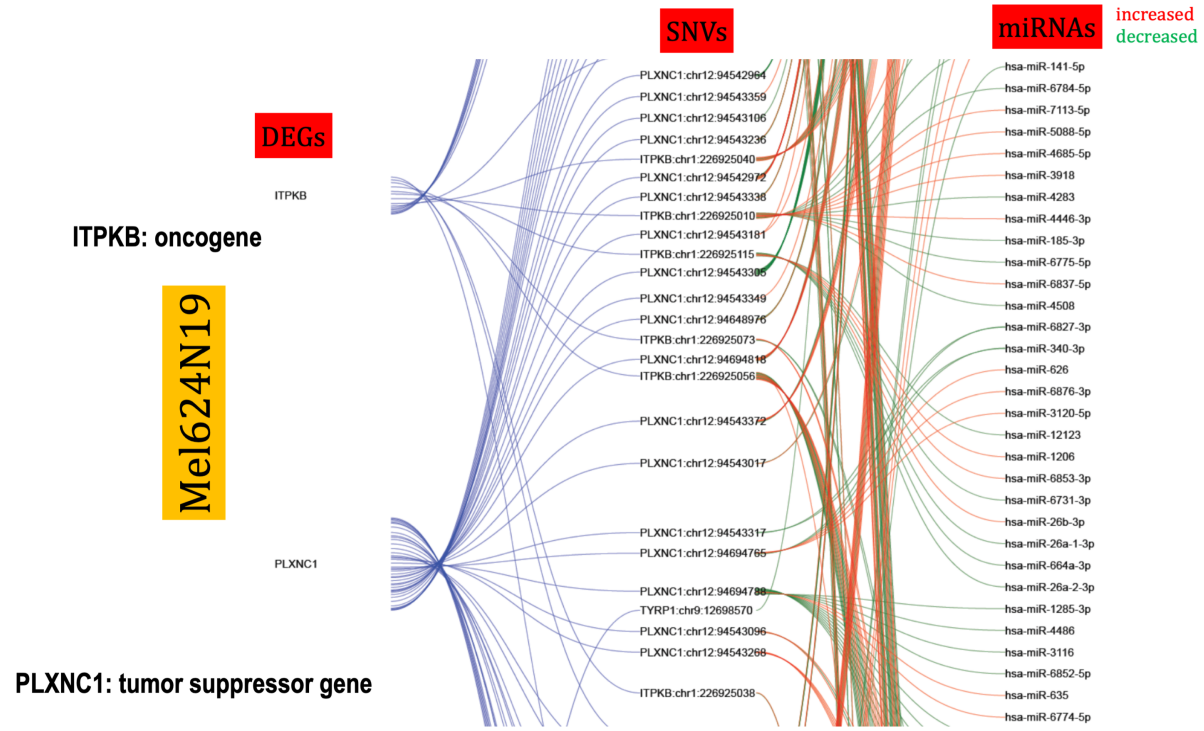

Figure 4.6. Integrated analysis (Mel624 N19)

ITPKB is an oncogene which—when up regulated—is associated with cisplatin resistance in ovarian cancer[88]. It is also known to be strongly up regulated in melanoma[89]. PLXNC1 is a tumor suppressor known to be involved in axon guidance, cell motility, and the immune response. One group suggested that PLXNC1 is a regulatory target of the long noncoding RNA CASC2[90]. Several synonymous SNVs are associated with each of these genes and each of those SNVs results in increased or decreased binding of miRNAs. Due to changes in miRNA binding—and consequentially mRNA stability—we expected to record changes in gene expression. We suspect that some of the transcriptional differences recorded between the parental lines and resistant library lines mentioned in Chapter 2 are due to changes in miRNA binding efficiency at the enriched SNV sites.

When investigating this phenomenon at a global level, we noticed that the SNVs in Mel624 tended to be under represented in Mel624N19. Alternatively, the SNVs in Mel888N19 tend to be under represented in Mel888. In Chapter 2 we highlighted how the gene expression profiles—though similar in the case of biologically relevant resistance genes—were different between the Mel624 and Mel888 cell lines. That being the case, the difference in SNVs between the parental lines and resistant library lines is expected. The two different cell lines are earmarking different passenger mutations for long term resistance and metastasis. These data are also consistent with the difference in VRT enrichment profiles mentioned in Chapter 2. If the VRTs are acting as sponges for other noncoding RNA molecules associated with the primary driver resistance genes, we should expect significant differences in which secondary passenger genes are impacted.

Integration of the whole exomic sequencing data with the RNAseq data showed that when the SNV alteration threshold was set to ± 12.5% only 75 genes were shared between Mel624N19 and Mel888N19 (Figure 4.7).

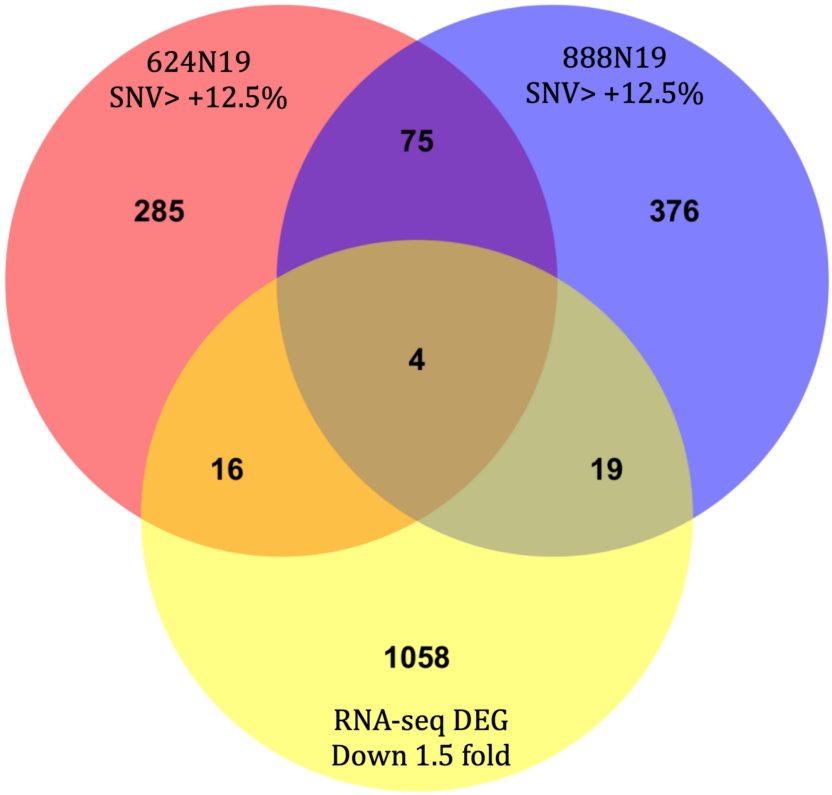

Figure 4.7. Integrated analysis SNVs >12.5% v DEG Down 1.5 fold

When adding the additional constraint of the differential gene expression being down regulated by 1.5 fold, there are only 4 genes in common.

Chapter 5

Summary, discussion, proposed mechanism, and future directions

5.1 Summary

Though far from the most deadly, cutaneous melanoma is an increasingly common neoplasm that afflicts both men and women all around the world. Understanding the molecular underpinnings of this disease is paramount. As our understanding of the epidemiology of melanoma improved, so did our ability to screen for and treat the disease in early stages. However, the metastasis associated with advanced disease is the major contributing factor to the high mortality rates associated with melanoma. Targeting the well characterized driver mutations —particularly the $BRAF^{V600E}$ mutation—was initially very promising. BRAFi showed improved progression free and overall survival rates with an associated decrease in systemic side effects. However, the clinical response was not durable and patients almost inevitably developed resistance to therapy. Discovering an answer for this important clinical problem required a different scientific approach to understanding melanoma drug resistance. In this thesis I explored noncoding RNA as a molecule of interest with regards to BRAFi resistance in melanoma.

In Chapter 2, I highlighted the different types of noncoding, regulatory RNA molecules to emphasize the variety of roles they serve in the cell. Most of what we understand about noncoding RNAs in cancer—particularly melanoma—is their role in tumorigenesis and metastasis. We hypothesized that regulatory RNA must also be involved in the resistance phenotype. Considering stability and ease of design, we decided to investigate their role using our synthetic N19 library with regulatory RNA molecules of 19 bases. Using a system previously

developed in our lab, allowed us to interrogate a wide range of molecules. Not only was our library capable of recapitulating resistance to vemurafenib in vitro, but that resistance was a result of clinically and biologically relevant up regulation of resistance genes. Since our library contains a vast number of regulatory molecules—upwards of $3x10^7$ transcripts—it was important for us to determine if there were any enriched molecules in the resistant cell population

In Chapter 3, we demonstrated that introduction of our library resulted in significant changes to the transcriptome of parental cell lines. This means that the resistance phenotype was established before treatment was initiated. The gene expression profile of the library cell lines were drastically different from the parental cell lines with and without treatment. Some of the most significant changes were in signaling pathways related to cell morphology, EMT, and growth and proliferation pathways. We noticed that some of the same genes were differentially expressed in both. These data indicated the significance of the molecular structure of the regulatory RNA. 23 genes were similarly regulated in the Mel624 cell line by the Mel624N19 library and the Mel624-888VRT1000 library. These data might highlight the genes that are integral to the resistance pathway regardless of the tumor sample. Data from KEGG plots helped to highlight not only growth and proliferation signaling pathways that are activated to compensate for BRAFi but also cell morphology and EMT genes that are activated in association with metastasis and invasion. Looking at these data help us see resistance is not simply related to evading treatment, but it is also related to traveling to a secondary niche.

We knew that the transcriptome of the library resistant lines was altered, but we were curious as to whether or not the genome was altered as well. Whole exomic sequencing completed in Chapter 4 revealed that there are number of mutational differences between the

parental lines and the library lines. These differences were realized across the genome. The more robust N19 library had a greater impact on the genome than the libraries generated from the single consensus sequence or enriched VRTs. Further investigation of the mutations revealed that the vast majority of them were synonymous mutations. This led us to ask what is the biological advantage that resistant cell populations gain from enriching for mutations in genes that do not result in a change in amino acid structure. We hypothesized that SNVs—even synonymous ones—might serve as binding sites for miRNAs that are involved in generating a resistance phenotype. Using bioinformatic techniques, we were able to link SNVs in several genes to differential binding of several possible miRNAs. Combining our whole exomic sequencing data and our RNAseq data for both N19 library cell lines allowed us to identify differentially expressed genes that also had changes in SNVs from the parental line to the resistant line.

5.2 Discussion

The goal of this thesis was to identify a network of regulatory RNAs responsible for the development of BRAFi resistance in melanoma. In order to accomplish that goal, we developed a novel noncoding RNA screening library. Our N19 library allowed us to screen upwards of $3x10^7$ unique 19bp long regulatory RNAs in a high throughout manner. By introducing so many 19mers to our parental cells, we were able to reduce screening bias. One potential concern about using a synthetic library was that the resulting phenotypes might not mimic what has been previously seen in the clinic. By intentionally designing the plasmid to create short transcripts under RNA Pol III promoters, we biased our library to create short regulatory RNAs. Stable expression of our library was associated with up regulation of canonical BRAFi resistance genes.

Additionally, we demonstrated that library cells maintained physiological ability to metastasize and resist BRAFi treatment over a range of doses. This library could potentially be used to interrogate the role of noncoding RNAs in other cancer drug resistance pathways.

One additional benefit of using our library approach was the ability to check for enrichment of certain species in the cell population and easily reintroduce a single enriched species to parental cell lines. We were able to very easily identify transcripts that we introduced to differentiate them from native noncoding RNA species. This gave us the ability to more closely link the resistant phenotype to the introduction of our library. Furthermore, taking enrichment into account helped us to construct a consensus sequence. The consensus VRT sequences took enrichment percentage into account. In doing so, we were able to investigate the contribution of overall structure of the transcript on the resistance phenotype. This is significant because consensus sequences can be generated from resistant cell populations with disperse enrichment profiles. It also shows the ability for a single noncoding RNA molecule to act in several different ways.

Generating a resistance phenotype requires coordinated gene expression over several loci. So, we expected that introducing our library would result in some changes in the transcriptome. The benefit to approaching this analysis with a large noncoding RNA library was being able to see changes to the transcriptome outside of the canonical resistance gene up regulation. It was significant that gene expression was altered even before BRAFi treatment was administered. This meant that the cell population was primed to respond to BRAFi. The heat map data demonstrated that resistance pathways might be on standby in melanoma from tumorigenesis. This conclusion was corroborated by the fact that cell morphology, EMT, and growth and proliferation pathways

were highlighted in the KEGG plot. The fact that the gene expression profile differed between the two cell lines might suggest that resistance phenotype might be slightly different from one patient to the next. In the future it might be useful to do introduce the library to ex vivo tumor cells from patients in order to better understand the resistance pathway.

The whole exomic sequencing data revealed SNVs throughout the genome. Were it not for the qPCR data showing resistance gene up regulation, we might have concluded that the library was random. After confirming that the majority of the SNVs were synonymous, the broad impact of the library suggested a cataloguing of passenger mutations. This was significant because it shed light on the potential utility of passenger mutations with regards to the resistance phenotype.

5.3 Proposed Mechanism

Introduction of our N19 library produces short noncoding RNAs which acts as a sponges for other noncoding RNA molecules like miRNAs. This results in differential mRNA expression which is responsible for generating the resistance phenotype. Establishing a stably resistant population is the result of passive enrichment and depletion of cells with beneficial SNVs. Those SNVs are associated with mRNA expression that is responsible for generating the resistant phenotype. Since SNVs might serve as binding sites for noncoding RNAs, we also propose that our library might act as a selective pressure for SNVs that contribute to the resistance phenotype.

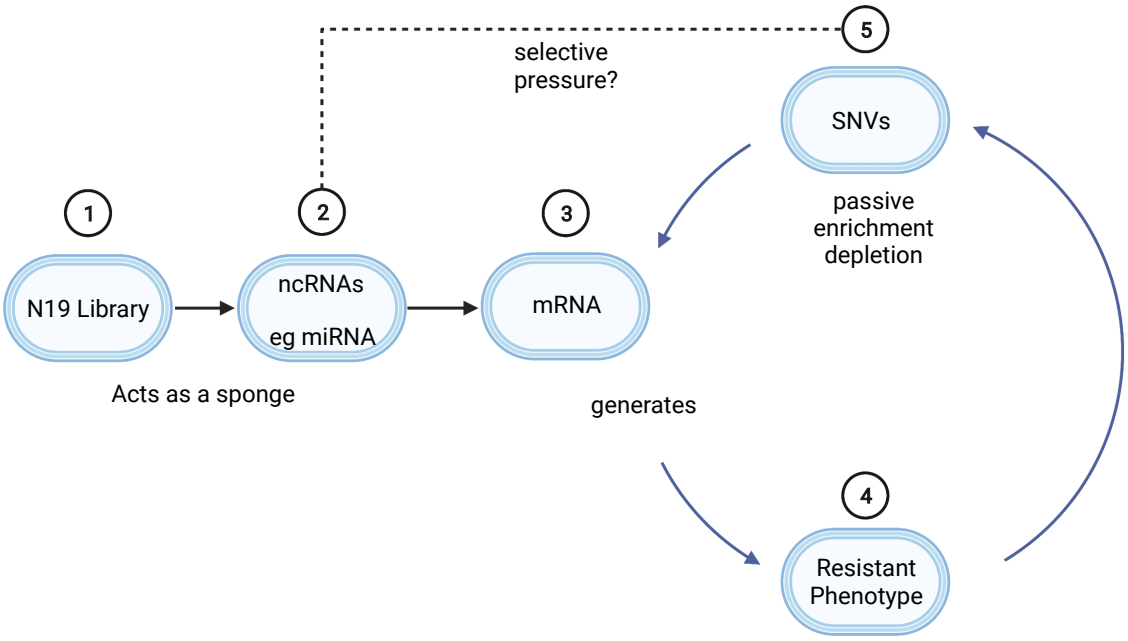

Figure 5.1. Potential mechanism of action

5.4 Future Directions

Though much about the nature of noncoding RNA in BRAFi resistance has been elucidated by this body of work, there are still several unanswered questions and ways this novel technology can be leveraged. We demonstrated the ability to recapitulate a biologically relevant BRAFi resistance phenotype in melanoma cells using the novel N19 library. In the future, that same library will be used to explore the resistance phenotype in combination therapy. We suspect different enrichment profiles with the addition of other molecules targeted the MAPK signaling pathway. Additionally, this library will be used to better understand resistance to immunotherapy. Another possible next step would be to implement this novel technology in an in vivo setting with both mouse and human melanoma cell lines. Doing so will certainly generate data that would be useful in the clinic. Delivering combinations of the enriched VRTs to melanoma cells would also shed valuable insight on downstream effects of introducing the library. The consensus VRT1000 sequences suggested an integral structural component to the noncoding transcripts that drove the resistance phenotype.

The next steps for chapter 3 will be to look further into the difference in baseline gene expression profiles between the Mel888 and Mel624 cell lines following the introduction of the N19 library. Comparing those expression profiles to profiles after the introduction of individual VRTs would also yield interesting data. Having identified some of the similarly regulated genes between cell lines, future studies will involve increased or decreased expression of those genes in order to generate more or less resistance to BRAFi. Perhaps specific new noncoding 19mers would be generated in order to specifically target those genes or their associated regulatory RNAs to investigate the impact on the resistance phenotype.

More robust studies of SNVs will be done using both individual VRTs and the consensus VRT1000 sequences. Using the Circa maps generated in chapter 4, future studies will be done to identify individual resistance genes that are either shared or are unique amongst different variations of the library. New individual VRTs would be designed in order to target specific genes in order to change the resistance phenotype. Many related miRNAs were identified in chapter 4. Future studies will be done to verify the changes in binding efficiency. Additionally, the library will be redesigned in order to target those particular miRNAs to see if there are any changes to the resistance phenotype as a result. Investigating the structural similarities between the enriched 19mers and the miRNAs associated with the SNVs might also help answer questions about whether or not introduction of our library directly acts as a selective pressure in the process of building the resistance phenotype. We will also complete more integrated analysis using individual VRTs and the VRT1000 consensus sequences in order to see the similarities and differences in differentially expressed genes, enriched SNVs, and related changes to miRNA binding efficiencies.

Chapter 6

Materials and Methods

Cell Culture and Chemicals

Mel624 and Mel888 cells were obtained from the American Type Culture Collection (ATCC, Manassas, VA). All cell lines were maintained in DMEM supplemented with 10% fetal bovine serum (FBS, Gemini Bio-Products, West Sacramento, CA), containing 100 U/mL penicillin and 100 μg/mL streptomycin, at 37 °C in 5% CO2. All restriction endonuclease enzymes were purchased from New England Biolabs (NEB, Ipswich, MA). Blasticidin S was purchased from InvivoGen (San Diego, CA). Unless indicated otherwise, other reagents were purchased from Sigma-Aldrich (St. Louis, MO) or Thermo Fisher Scientific (Waltham, MA).

Construction of BstXI-Based Shotgun (BSG) Multiplex siRNA Expression System

The entry vectors pBSG361A/B/ C were first engineered on the base of pBR322 plasmid so that each vector contains the converging U6−H1 promoters to drive siRNA expression with unique restriction sites for the subcloning of siRNA oligo cassettes (SiOCs), whereas the U6−H1-driven siRNA expression units (SiEUs) were flanked with a pair of distinct BstXI sites, namely BstXI-A and BstXI-B in pBSG361A, BstXI-B and BstXI-C in pBSG361B, and BstXI-C and BstXI-D in pBSG361C, respectively. A retroviral destination vector, pSEB361-BSG, was also engineered for shotgun cloning of multiple BstXI-digested SiEUs from the pBSG361 vectors at the BstXI-A and BstXI-D sites.

The siRNA sites targeting the coding regions of mouse β- catenin (NM_007614.3) and Smad4 (NM_008540.3) were designed by using the BLOCK-iT RNAi Designer (Invitrogen, Carlsbad, CA) and/or the siDESIGN programs (Dharmacon, Lafayette, CO), as previously described.14,16−18 Three scrambled oligo sequences, which do not target any significant known human and rodent transcripts, were used as controls, or siControl. The annealed siRNA oligo cassettes (Supplemental Table 1) were used for shotgun cloning into the pBSG361 entry vectors. The resulting constructs were designated as pBSG361- simBC-A/B/C (for mouse β-catenin siRNAs) and pBSG361- simSmad4-A/B/C (for mouse Smad4 siRNAs), as well as pBSG361-simBC/Smad4 for the dual targeting siRNAs of β- catenin/Smad4, and pBSG361-siControl. To construct a multiplex siRNA expression retroviral vector, the three corresponding SiEUs were isolated from pBSG361 vectors by BstXI digestion, and pooled for shotgun ligation into the BstXI- A/BstXI-D sites of the pSEB361-BSG retroviral vector. All cloned oligo cassettes were verified by DNA sequencing. Details about the construction of these vectors and related vector sequences are available upon request.

Establishment of Stable siRNA Expressing Cell Lines of Mesenchymal Stem Cells iMEFs

The retroviral transfer vectors pSEB361-simBC, pSEB361-simSmad4, pSEB361-simBC/Smad4, and pSEB361-siControl were cotransfected with retroviral packaging plasmids into the 293 Phoenix Ampho (293PA) cells to generate retrovirus supernatants for infecting subconfluent iMEF cells as previously described. At 36−48 h post-viral-infection, the cells were subjected to blasticidin S selection (final concentration at 3 μg/mL) for 5 days. The resultant stable lines were designated as iMEF-simBC, iMEF-simSmad4, iMEF-simBC/Smad4, and iMEF-siControl, respectively.

Bacterial Colony PCR Screening Assay

Ligation products were transformed into aliquots (usually 5−10 μL) of electro-competent DH10B cells (NEB) via electroporation and directly plated onto LB/agar/Kan or Amp plates, as described.63,76,77 Bacterial colonies were grown for 14−16 h in a 37 °C incubator. Colony PCR was performed as described.76,77 Briefly, PCR master mix (usually 10−20 μL/reaction) was first aliquoted into a 96-well PCR plate (or multiple 8-tube strips for PCR). At the same time, a replicate of a sterile 96-well cell culture plate was set up by adding ~50 μL/well LB/Amp or LB/Kap medium. Bacterial colonies were then carefully picked up with sterile p200 pipet tips and loaded onto a 12- or 8-channel pipet. The colony-containing tips were first rinsed gently in the 96-well culture plate loaded with LB/Amp or LB/Kam culture medium, and then rinsed in the corresponding wells of the PCR plate. The LB plate was moved to a 37 °C bacterial incubator, whereas the PCR plate was used for 26−28 cycles of PCR amplification. The PCR products were resolved on 1% agarose gels. Bacterial culture medium corresponding to positive PCR results was grown up for plasmid DNA preparations and further confirmation by PCR, restriction digestion, and/or DNA sequencing.

Crystal Violet Staining

Crystal violet staining assay was conducted as described [25-28]. Briefly, subconfluent HeyA8- MDR, OVCAR8-PR29A and/or OVCAR8-PR29B cells were treated with varied concentrations of DMSO, PTX, and/or vemurafenib (VEM). At 72 h after treatment, the cells were washed with PBS and stained with 0.5% crystal violet/for- malin solution at room temperature for 20-30 min. The stained cells were rinsed with tape water, air-dried, and documented by a photoscanner

RNA isolation and quantitative PCR analysis

Total RNA was extracted by using the TRIZOL reagent (Invitrogen, Carlsbad, CA) according to the manufacturer's protocol and subjected to reverse transcription reactions using hexam- er and M-MuLV Reverse Transcriptase (New England Biolabs, Ipswich, MA). The resultant cDNA products were diluted 10- to 100-fold and used as PCR templates. PCR primers were designed by using the Primer3 Plus program [35]. All qPCR primer sequences are listed in Supplementary Table 1. The quantitative PCR analysis was carried out by using our previously optimized TqPCR protocol [23, 36-43]. Briefly, the 2x SYBR Green qPCR reactions (Bimake, Houston, TX) were set up according to manu- facturer's instructions. The cycling program was modified by incorporating 4 cycles of touchdown steps prior to the regular cycling program. GAPDH was used as a reference gene. All sample values were normalized to GAPDH expression by using the 2-ΔΔCt method.

Cell transfection

For the reported studies, freshly seeded subconfluent cells were transfected by using the linear polyethylenimine (PEI)-based Transporter 5™ Transfection Reagent (Polysciences, Inc., Warrington, PA) according to the manufacturer's instructions. At the indicated time points, the transfected cells were collected for various assays described below.

Total RNA isolation and touchdown quantitative real-time PCR (TqPCR)

At the endpoint, the transfected cells were subjected to total RNA isolation by using NucleoZOL Reagent (Takara Bio USA, Mountain View, CA) according to the manufacturer's introduction. For qPCR analysis of mRNA transcripts, total RNA was used for reverse transcription with the hexamer and M-MuLV (NEB). The cDNA products were diluted as

templates for qPCR. The qPCR primers were designed by Primer3 Plus program [48]. For assessing the miR expression levels mediated by the three expression systems, the reverse transcription reactions were carried out by using miR-specific reverse primers that were complementary with the 3′-end six nucleotides of mature miR-5p and/or miR-3p, preceded with a 44-nt artificial stem-loop sequence. SYBR green-based quantitative real-time PCR analysis was performed by following our previously optimized TqPCR protocol [49]. The qPCR reactions were done in triplicate. All expression values were normalized to the reference gene GAPDH expression by using the 2–ΔΔCt method [50,51,52,53]. The sequences of the qPCR primers are listed in Supplemental Table

Cell cycle analysis

Cell cycle analysis was conducted as previously described [57, 66, 67]. Exponentially growing HEK-293 and HCT116 cells were seeded in 60 mm dishes and transfected with let-7a-1 expression plasmids or vector control. At 48 h post transfection, cells were collected and stained with the Magic Solution (containing 0.05% NP-40, 4% formaldehyde, 0.01 μg/ml Hoechst 33258 in PBS) for 30 min [68]. The stained cells were subjected to flow cytometry analysis using BD FACSCalibur-HTS. The flow cytometry data were quantitatively analyzed by FlowJo software. Each assay condition was performed in triplicate.

DNA and RNA extraction

Fresh-frozen tumor DNA was extracted using the AllPrep® DNA/RNA/miRNA Universal kit (Qiagen #80224) for both DNA and RNA extraction. Blood DNA was extracted from whole blood using the QIAamp® DNA Blood Kit (#51126). DNA samples were quantified using a NanoDrop (ND1000, Thermoscientific) and Qubit® dsDNA HS Assay (Q32851, Life

Technologies) with DNA size and quality tested using gel electrophoresis. RNA samples were quantified using the Qubit® RNA HS Assay (Q32852, Life Technologies). Most DNA and RNA samples were from the same vial of tissue. Six RNA-seq (MELA_0267, MELA_0015, MELA_0004, MELA_0268, MELA_0068, MELA_0010) samples were the same lesion, but from a different vial of tissue than the DNA sample.

Whole-genome sequencing

Sequencing library construction was performed using TruSeq DNA Sample Preparation kits (Illumina, San Diego, California, USA) according to the manufacturer's instructions. Whole-genome paired-end sequencing was performed on HiSeq2000, HiSeq X Ten or NovaSeq instruments (Illumina, San Diego, CA, USA) at the Kinghorn Cancer Centre, Garvan Institute of Medical Research (Sydney, Australia) or Macrogen (Geumcheon-gu, Seoul, South Korea). Tumor samples underwent whole genome sequencing to a median coverage of 59X (range 35–118) and normal germline samples to a median coverage of 35X (range 21–124). Sequenced data was adapter trimmed using Cutadapt53 (version 1.9) and aligned to the GRCh37 assembly using BWA-MEM54 (version 0.7.12) and SAMtools55 (version 1.1). Duplicate reads were marked with Picard MarkDuplicates (https://broadinstitute.github.io/picard, version 1.129). Tumor purity was assessed using ascatNGS56 and all tumors had a minimum purity of 35%.

RNA sequencing analysis

Libraries were prepared from RNA using the TruSeq Stranded mRNA kit and sequenced with 100 bp paired end reads. RNA-seq reads were aligned using STAR (version 2.5.2a)57 to the GRCh37 assembly with the gene, transcript, and exon features of Ensembl (release 70) gene model after trimming for adapter sequences using Cutadapt (version 1.9). Quality control metrics

were computed using RNA-SeQC (version 1.1.8)58 and gene expression was estimated using RSEM (version 1.2.30)59. Samples were TMM (trimmed mean of M values) normalized using the R package edgeR60 and for expression comparisons of samples with and without gene mutations of interest and for PD-L1 (CD274) expression, log2(TMM normalized counts +1) were used. Immune cell deconvolution of the tumor micro-environment was estimated using CIBERSORT61. The algorithm was run for 500 permutations using TPM values from RSEM as input with the supplied LM22 (22 immune genes) gene signature file and, as recommended, quantile normalization was disabled.

Somatic substitution and indel calling

Somatic SNV and indels were detected using an established pipeline13. A dual calling strategy was used to detect SNVs/DNVs/TNVs, with the consensus of two different tools being used for downstream analysis: qSNP (version 2.0)62 and GATK HaplotypeCaller (version 3.3-0)63. Detection of indels (1–50 bp) was carried out using GATK. SnpEff64 was used to perform variant annotation for gene consequence. Kataegis regions of localized hypermutation were determined using previously established metrics13. Inter-mutational distances (the number of base pairs between mutations) were segmented using piecewise constant fitting and putative regions of kataegis were defined as those segments that contained six or more consecutive mutations with a mean inter-mutation distance of ≤1000 bp.

Endnotes

[1] Goldsmith, L., et al. "Fitzpatrick's Dermatology in General Medicine, Ed." *McGraw Hill Medical* 150.4 (2012): 22.

[2] D'Mello, Stacey AN, et al. "Signaling pathways in melanogenesis." *International journal of molecular sciences* 17.7 (2016): 1144.

[3] Cichorek, Mirosława, et al. "Skin melanocytes: biology and development." Advances in Dermatology and Allergology/Postępy Dermatologii i Alergologii 30.1 (2013): 30-41.

[4] Maddodi, Nityanand, Ashika Jayanthy, and Vijayasaradhi Setaluri. "Shining light on skin pigmentation: the darker and the brighter side of effects of UV radiation." *Photochemistry and photobiology* 88.5 (2012): 1075-1082.

[5] Schadendorf, Dirk, et al. "Melanoma." *The Lancet* 392.10151 (2018): 971-984.

[6] Eggermont, Alexander MM, Alan Spatz, and Caroline Robert. "Cutaneous melanoma." *The Lancet* 383.9919 (2014): 816-827.

[7] American Cancer Society. Cancer Statistics Center. http://cancerstatisticscenter.cancer.org. Accessed June 7, 2022.

[8] Bolognia, Jean L., Joseph L. Jorizzo, and Julie V. Schaffer. Dermatology e-book. Elsevier Health Sciences, 2012.

[9] Goydos, James S., and Steven L. Shoen. "Acral lentiginous melanoma." Melanoma (2016): 321-329.

[10] Menzies, Scott W., et al. "Dermoscopic evaluation of nodular melanoma." JAMA dermatology 149.6 (2013): 699-709.

[11] Gershenwald, Jeffrey E., and Richard A. Scolyer. "Melanoma staging: American joint committee on cancer (AJCC) and beyond." *Annals of surgical oncology* 25.8 (2018): 2105-2110.

[12] Potrony, Miriam, et al. "Update in genetic susceptibility in melanoma." Annals of translational medicine 3.15 (2015).

[13] Ascierto, Paolo A., et al. "The role of BRAF V600 mutation in melanoma." Journal of translational medicine 10.1 (2012): 1-9.

[14] Kelleher, Fergal C., and Grant A. McArthur. "Targeting NRAS in melanoma." The Cancer Journal 18.2 (2012): 132-136.

[15] Pham, Duc Daniel M., Samantha Guhan, and Hensin Tsao. "KIT and melanoma: biological insights and clinical implications." *Yonsei medical journal* 61.7 (2020): 562.

[16] Scatena, Cristian, Daniela Murtas, and Sara Tomei. "Cutaneous melanoma classification: the importance of high-throughput genomic technologies." *Frontiers in oncology* (2021): 1313.

[17] Slipicevic, Ana, and Meenhard Herlyn. "KIT in melanoma: many shades of gray." *Journal of Investigative Dermatology* 135.2 (2015): 337-338.

[18] Wiesner, Thomas, et al. "NF1 mutations are common in desmoplastic melanoma." *The American journal of surgical pathology* 39.10 (2015): 1357.

[19] Kiuru, Maija, and Klaus J. Busam. "The NF1 gene in tumor syndromes and melanoma." *Laboratory investigation* 97.2 (2017): 146-157.

[20] Halaban, Ruth. "RAC1 and melanoma." *Clinical therapeutics* 37.3 (2015): 682-685.

[21] Huang, Franklin W., et al. "Highly recurrent TERT promoter mutations in human melanoma." Science 339.6122 (2013): 957-959.

[22] Hugdahl, Emilia, et al. "Prognostic impact and concordance of TERT promoter mutation and protein expression in matched primary and metastatic cutaneous melanoma." British journal of cancer 118.1 (2018): 98-105.

[23] Hartman, Mariusz L., and Malgorzata Czyz. "Anti-apoptotic proteins on guard of melanoma cell survival." *Cancer letters* 331.1 (2013): 24-34.

[24] Mitra, Devarati, and David E. Fisher. "Transcriptional regulation in melanoma." *Hematology/ Oncology Clinics* 23.3 (2009): 447-465.

[25] Garraway, Levi A., et al. "Integrative genomic analyses identify MITF as a lineage survival oncogene amplified in malignant melanoma." *Nature* 436.7047 (2005): 117-122.

[26] Widlund, Hans R., et al. "β-Catenin–induced melanoma growth requires the downstream target Microphthalmia-associated transcription factor." *The Journal of cell biology* 158.6 (2002): 1079-1087.

[27] Hodis, Eran, et al. "A landscape of driver mutations in melanoma." *Cell* 150.2 (2012): 251-263.

[28] Colombino, Maria, et al. "BRAF/NRAS mutation frequencies among primary tumors and metastases in patients with melanoma." *J Clin Oncol* 30.20 (2012): 2522-2529.

[29] Rozenberg, Gabriela I., et al. "Metastasis in an orthotopic murine model of melanoma is independent of RAS/RAF mutation." *Melanoma research* 20.5 (2010): 361.

[30] Jakob, John A., et al. "NRAS mutation status is an independent prognostic factor in metastatic melanoma." *Cancer* 118.16 (2012): 4014-4023.

[31] Zhou, Xiao-Ping, et al. "Epigenetic PTEN silencing in malignant melanomas without PTEN mutation." *The American journal of pathology* 157.4 (2000): 1123-1128.

[32] Ko, Justin M., Nicole F. Velez, and Hensin Tsao. "Pathways to melanoma." *, 29, 4* 29.4 (2010): 210-217.

[33] Stahl, Jill M., et al. "Deregulated Akt3 activity promotes development of malignant melanoma." *Cancer research* 64.19 (2004): 7002-7010.

[34] Dankort, David, et al. "BrafV600E cooperates with Pten loss to induce metastatic melanoma." *Nature genetics* 41.5 (2009): 544-552.

[35] Nogueira, Cristina, et al. "Cooperative interactions of PTEN deficiency and RAS activation in melanoma metastasis." *Oncogene* 29.47 (2010): 6222-6232.

[36] Deng, Wentao, et al. "WNT1-inducible signaling pathway protein 1 (WISP1/CCN4) stimulates melanoma invasion and metastasis by promoting the epithelial–mesenchymal transition." *Journal of Biological Chemistry* 294.14 (2019): 5261-5280.

[37] Bedogni, Barbara. "Notch signaling in melanoma: interacting pathways and stromal influences that enhance Notch targeting." *Pigment cell & melanoma research* 27.2 (2014): 162-168.

[38] Davis, Lauren E., Sara C. Shalin, and Alan J. Tackett. "Current state of melanoma diagnosis and treatment." Cancer biology & therapy 20.11 (2019): 1366-1379.

[39] Patel, Hima, et al. "Current advances in the treatment of BRAF-mutant melanoma." Cancers 12.2 (2020): 482.

[40] Liu, Yuxin, and M. Saeed Sheikh. "Melanoma: molecular pathogenesis and therapeutic management." Molecular and cellular pharmacology 6.3 (2014): 228.

[41] Domingues, Beatriz, et al. "Melanoma treatment in review." ImmunoTargets and therapy 7 (2018): 35.

[42] Bhatia, Shailender, Scott S. Tykodi, and John A. Thompson. "Treatment of metastatic melanoma: an overview." Oncology (Williston Park, NY) 23.6 (2009): 488.

[43] Das Thakur, Meghna, et al. "Modelling vemurafenib resistance in melanoma reveals a strategy to forestall drug resistance." Nature 494.7436 (2013): 251-255.

[44] Straussman, Ravid, et al. "Tumour micro-environment elicits innate resistance to RAF inhibitors through HGF secretion." Nature 487.7408 (2012): 500-504.

[45] Proietti, Ilaria, et al. "Mechanisms of acquired BRAF inhibitor resistance in melanoma: a systematic review." Cancers 12.10 (2020): 2801.

[46] Kelleher, Fergal C., and Grant A. McArthur. "Targeting NRAS in melanoma." The Cancer Journal 18.2 (2012): 132-136.

[47] Zhao, Yujie, and Alex A. Adjei. "The clinical development of MEK inhibitors." Nature reviews Clinical oncology 11.7 (2014): 385-400.

[48] Grimaldi, Antonio M., Ester Simeone, and Paolo A. Ascierto. "The role of MEK inhibitors in the treatment of metastatic melanoma." Current opinion in oncology 26.2 (2014): 196-203.

[49] Lugowska, Iwona, Pawel Teterycz, and Piotr Rutkowski. "Immunotherapy of melanoma." Contemporary Oncology/Współczesna Onkologia 2018.1 (2018): 61-67.

[50] Robert, Caroline. "A decade of immune-checkpoint inhibitors in cancer therapy." Nature Communications 11.1 (2020): 1-3.

[51] Klemen, Nicholas D., et al. "Patterns of failure after immunotherapy with checkpoint inhibitors predict durable progression-free survival after local therapy for metastatic melanoma." *Journal for immunotherapy of cancer* 7.1 (2019): 1-9.

[52] Winkle, Melanie, et al. "Noncoding RNA therapeutics—Challenges and potential solutions." Nature reviews Drug discovery 20.8 (2021): 629-651.

Zhang, Peijing, et al. "Non-coding RNAs and their integrated networks." *Journal of integrative bioinformatics* 16.3 (2019).

[54] Chan, Jia Jia, and Yvonne Tay. "Noncoding RNA: RNA regulatory networks in cancer." *International journal of molecular sciences* 19.5 (2018): 1310.

[55] Khaitan, Divya, et al. "The Melanoma-Upregulated Long Noncoding RNA SPRY4-IT1 Modulates Apoptosis and InvasionNoncoding RNA Function SPRY4-IT1 in Human Melanoma." Cancer research 71.11 (2011): 3852-3862.

[56] Schmidt, Karyn, et al. "The lncRNA SLNCR1 mediates melanoma invasion through a conserved SRA1-like region." Cell reports 15.9 (2016): 2025-2037.

[57] Díaz-Martínez, Marta, et al. "miR-204-5p and miR-211-5p Contribute to BRAF Inhibitor Resistance in MelanomamiRNA Contribution to BRAF Inhibitor Melanoma Resistance." Cancer research 78.4 (2018): 1017-1030.

[58] Yu, Xin, et al. "Long non-coding RNAs in melanoma." Cell proliferation 51.4 (2018): e12457.

[59] Leucci, Eleonora, et al. "Melanoma addiction to the long non-coding RNA SAMMSON." Nature 531.7595 (2016): 518-522.

[60] Chen, Xiang-jun, et al. "Regulation of melanoma malignancy by the RP11-705C15. 3/miR-145-5p/NRAS/MAPK signaling axis." Cancer gene therapy 28.10 (2021): 1198-1212.

[61] Balas, Maggie M., and Aaron M. Johnson. "Exploring the mechanisms behind long noncoding RNAs and cancer." Non-coding RNA research 3.3 (2018): 108-117.

[62] Gajos-Michniewicz, Anna, Markus Duechler, and Malgorzata Czyz. "MiRNA in melanoma-derived exosomes." Cancer letters 347.1 (2014): 29-37.

[63] Xu, Wen, and Grant McArthur. "Cell cycle regulation and melanoma." Current oncology reports 18.6 (2016): 1-12.

[64] Reddy, Bobby Y., David M. Miller, and Hensin Tsao. "Somatic driver mutations in melanoma." Cancer 123.S11 (2017): 2104-2117.

[65] Brabletz, Thomas, et al. "EMT in cancer." Nature Reviews Cancer 18.2 (2018): 128-134.

[66] Nieto, M. Angela, et al. "EMT: 2016." Cell 166.1 (2016): 21-45.

[67] Satelli, Arun, and Shulin Li. "Vimentin in cancer and its potential as a molecular target for cancer therapy." Cellular and molecular life sciences 68.18 (2011): 3033-3046.

[68] Hargadon, Kristian M., et al. "The FOXC2 transcription factor promotes melanoma outgrowth and regulates expression of genes associated with drug resistance and interferon responsiveness." Cancer Genomics & Proteomics 16.6 (2019): 491-503.

[69] Wang, Yifan, et al. "The role of snail in EMT and tumorigenesis." Current cancer drug targets 13.9 (2013): 963-972.

[70] Weiss, Michele B., et al. "TWIST1 Is an ERK1/2 Effector That Promotes Invasion and Regulates MMP-1 Expression in Human Melanoma CellsERK1/2–TWIST1–MMP-1 Invasion Axis in Melanoma." Cancer research 72.24 (2012): 6382-6392.

[71] Czyz, Malgorzata. "HGF/c-MET Signaling in Melanocytes and Melanoma." International journal of molecular sciences 19.12 (2018): 3844.

[72] Kozar, Ines, et al. "Impact of BRAF kinase inhibitors on the miRNomes and transcriptomes of melanoma cells." *Biochimica et Biophysica Acta (BBA)-General Subjects* 1861.11 (2017): 2980-2992.

[73] Hoek, Keith S., et al. "Novel MITF targets identified using a two-step DNA microarray strategy." *Pigment cell & melanoma research* 21.6 (2008): 665-676.

[74] Bell, Rachel E., and Carmit Levy. "The three M's: melanoma, microphthalmia-associated transcription factor and microRNA." *Pigment cell & melanoma research* 24.6 (2011): 1088-1106.

[75] Zhang, Maoduo, et al. "TGF-β signaling and resistance to cancer therapy." *Frontiers in cell and developmental biology* 9 (2021).

[76] Brunen, Diede, et al. "TGF-β: an emerging player in drug resistance." *Cell cycle* 12.18 (2013): 2960-2968.

[77] Ahrens, Theresa D., et al. "The role of proteoglycans in cancer metastasis and circulating tumor cell analysis." *Frontiers in cell and developmental biology* 8 (2020): 749.

[78] Price, Matthew A., et al. "CSPG4, a potential therapeutic target, facilitates malignant progression of melanoma." *Pigment cell & melanoma research* 24.6 (2011): 1148-1157.

[79] Hu, Lei, et al. "Biglycan stimulates VEGF expression in endothelial cells by activating the TLR signaling pathway." *Molecular oncology* 10.9 (2016): 1473-1484.

[80] Xu, Jian, Samy Lamouille, and Rik Derynck. "TGF-β-induced epithelial to mesenchymal transition." *Cell research* 19.2 (2009): 156-172.

[81] Choe, Min Ho, et al. "miR-550a-3-5p acts as a tumor suppressor and reverses BRAF inhibitor resistance through the direct targeting of YAP." *Cell death & disease* 9.6 (2018): 1-12.

[82] Kurz, Susanne, et al. "The anti-tumorigenic activity of A2M—A lesson from the naked mole-rat." *PloS one* 12.12 (2017): e0189514.

[83] Shrestha, Yashaswi, et al. "PAK1 is a breast cancer oncogene that coordinately activates MAPK and MET signaling." *Oncogene* 31.29 (2012): 3397-3408.

[84] Da Vià, Matteo Claudio, et al. "CIC mutation as a molecular mechanism of acquired resistance to combined BRAF-MEK inhibition in extramedullary multiple myeloma with central nervous system involvement." *The oncologist* 25.2 (2020): 112-118.

[85] Adams, David J., David Timothy Bishop, and Carla Daniela Robles-Espinoza. "Melanoma predisposition—A limited role for germline BRCA1 and BRCA2 variants." *Pigment Cell & Melanoma Research* 33.1 (2020): 6-7.

[86] Yang, Qiuan, et al. "Comprehensive analyses of PBRM1 in multiple cancer types and its association with clinical response to immunotherapy and immune infiltrates." *Annals of Translational Medicine* 9.6 (2021).

[87] Nicoloso, Milena S., et al. "Single-nucleotide polymorphisms inside microRNA target sites influence tumor susceptibility." *Cancer research* 70.7 (2010): 2789-2798.

[88] Li, Jie, et al. "ROS-regulated phosphorylation of ITPKB by CAMK2G drives cisplatin resistance in ovarian cancer." *Oncogene* 41.8 (2022): 1114-1128.

[89] Avagliano, Angelica, et al. "Metabolic plasticity of melanoma cells and their crosstalk with tumor microenvironment." *Frontiers in Oncology* 10 (2020): 722.

[90] Wang, Zhiqiong, et al. "Long non-coding RNA CASC2 inhibits tumorigenesis via the miR-181a/PLXNC1 axis in melanoma." *Acta biochimica et biophysica Sinica* 50.3 (2018): 263-272.